# CHARACTERIZATION OF THE NORSPERMIDINE/SPERMIDINE TRANSPORT PROTEIN, POTD1, IN *VIBRIO CHOLERAE*

A Thesis

by

ALEXANDRIA COLETT RUTKOVSKY

Submitted to the Graduate School

Appalachian State University

in partial fulfillment of the requirements for the degree of

MASTERS IN SCIENCE

August 2012

Biology Department

CHARACTERIZATION OF THE NORSPERMIDINE/SPERMIDINE TRANSPORT PROTEIN, POTD1, IN *VIBRIO CHOLERAE*

A Thesis
by
ALEXANDRIA COLETT RUTKOVSKY
August 2012

APPROVED BY:

Dr. Ece Karatan
Chairperson, Thesis Committee

Dr. Susan Edwards
Member, Thesis Committee

Dr. Annkatrin Rose
Member, Thesis Committee

Dr. Steve Seagle
Chairperson, Department of Biology

Dr. Edelma Huntley
Dean, Research and Graduate Studies

ABSTRACT

CHARACTERIZATION OF THE NORSPERMIDINE/SPERMIDINE TRANSPORT PROTEIN, POTD1, IN *VIBRIO CHOLERAE*

Alexandria Colett Rutkovsky, B.S., Appalachian State University

M.S., Appalachian State University

Chairperson: Dr. Ece Karatan

Biofilm formation plays a large role in antibiotic resistance among bacteria and therefore proves to be an imperative avenue of research for future therapies. To combat biofilm formation, we must have a thorough understanding of all of the proteins and molecules that have an effect on biofilm formation. One such protein, PotD1, has been previously shown to negatively regulate biofilm formation in *Vibrio cholerae*, an aquatic bacterium which is also an intestinal pathogen. This protein was identified as the periplasmic ligand binding protein of the putative ATP-binding cassette transporter PotABCD1 and was shown to be responsible for uptake of the polyamine spermidine into *V. cholerae*. The purpose of this study was to biochemically characterize the PotD1 protein further. Overall, this work focused to understand the binding properties of the PotD1 protein to its ligands and ultimately its effect on biofilm formation in *V. cholerae* through genetic characterization of the ligand binding cleft and the ability of PotD1 to interact with various polyamines which have the potential to alter biofilm levels in this bacterium. The results demonstrated that in addition to spermidine, PotD1 is also responsible for the import of a closely related polyamine, norspermidine. Since no norspermidine transporters

have been identified to date in any organism, the PotABCD1 transporter is the first example of a norspermidine transporter. Ligand competition assays showed PotD1 has a higher binding affinity for spermidine rather than norspermidine. In addition, this work showed that the amino acids W252 and D254, hypothesized to be within the PotD1 ligand binding cleft, play a large role in spermidine transport, and the amino acids E168 and W32 play a less important role. The importance of these same amino acids in norspermidine transport are currently unknown, but experiments to determine this are underway. Lastly, mutations in the amino acids that diminished spermidine import only had a partial effect on biofilm formation, suggesting that spermidine uptake and biofilm formation are only partially correlated. Thus, this work also demonstrates the ability of PotD1 to alter biofilm formation by both its ability to uptake spermidine but also through another yet unidentified mechanism.

DEDICATION

This work is dedicated to my loving family who has taught me that persistence and focus will always pave the way to my dreams and aspirations.

ACKNOWLEDGMENTS

I would like to acknowledge the Appalachian State University Office of Student Research and Graduate Student Association for contributing to the funding in support of this research. This research was also supported in part by the Grant Number AI096358 from the National Institute of Allergy and Infectious Diseases awarded to Dr. Ece Karatan. I would like to thank the Karatan lab, both past and present, which has been instrumental in completion of this research. Thanks to members on my committee for offering creative advice and ideas, and special thanks to my advisor Dr. Ece Karatan for her constant patience, support, guidance, and wealth of knowledge.

TABLE OF CONTENTS

LIST OF TABLES

LIST OF FIGURES

# INTRODUCTION

*Vibrio cholerae* is an intestinal pathogen that thrives in aquatic environments by forming biofilms which allow the bacterium to survive otherwise harmful conditions. A biofilm is a surface aggregation of microorganisms in a complex, self-produced matrix. Biofilms are thought to aid the infectivity of *V. cholerae*, as well as other microbes, by providing protection from the host's natural defense mechanisms, thereby increasing the survival rates of bacteria (1, 2). The biofilm matrix is composed of sugars, proteins, and DNA, and encases the microorganisms, allowing an unparalleled form of protection from chemical and physical stresses (3, 4, 5). Following ingestion, *V. cholerae* is thought to colonize the small intestine by means of chemotaxis (6). Biofilm formation is important in aiding colonization of the host intestine by offering protection from the harsh environmental conditions encountered at the gastric acid barrier before entering the small intestine of the human host (1, 7). In addition, the physiological state of *V. cholerae*, while present in a biofilm and after exiting a biofilm, has been shown to contribute to infectivity (8, 9, 10). The biofilm phenotype of *V. cholerae* can be regulated by various environmental signals through the stringent control of complex regulatory systems that ensure the proper phenotype in the right environment (11). This work focuses on understanding how small cationic molecules, polyamines, are acquired and utilized by *V. cholerae* to influence biofilm formation.

Polyamines play a crucial role in optimal cell performance by regulating a variety of cellular processes such as regulation of transcription and translation, virulence, stress tolerance, and biofilms (12, 13, 14, 15, 16, 17, 18). Their ability to work in conjunction with

the regulatory machinery of the cell allows polyamines to act as inhibitors or promoters for a variety of regulatory processes by influencing specific proteins, mRNA, or DNA (19, 20, 21, 22, 23). Almost all cell types possess polyamine synthesis and transport systems to adjust the levels of various polyamines such as cadaverine, norspermidine, putrescine, and spermidine in the cell. In *V. cholerae*, polyamine synthesis and transport systems have been shown to play an especially large role in biofilm formation (24, 12). Previous results have confirmed a relationship between a decrease in biofilm formation with the presence of the polyamine spermidine. Similar experiments have also suggested that an increase in biofilm formation correlates with an increase in cellular and extracellular norspermidine levels. This is especially interesting considering norspermidine and spermidine differ by only one methylene group (Figure 1).

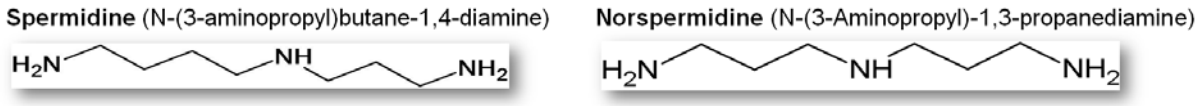


**Figure 1**. **Polyamines affecting biofilm formation in *V. cholerae*.** Spermidine and norspermidine differ by one methylene group.

The characteristics of polyamine transport vary in different prokaryotes. In *V. cholerae*, there is thought to be a PotABCD1 spermidine uptake system coded for by a gene cluster consisting of *potA*, *potB*, *potC*, *potD2*, and *potD1* genes, respectively (Figure 2), which belong to the ATP binding (ABC) cassette transporter family. ABC transporters are diverse and plentiful among many species. They are characterized by a certain design which incorporates at least two transmembrane domains (TMDs) and two nucleotide binding domains (NBDs). ABC transporters can function as excretion mechanisms in both eukaryotic and prokaryotic systems, but their ability to act as importers are generally exclusive to

prokaryotic organisms and require high affinity binding proteins, like the PotD1 protein in the PotABCD2D1 system, to deliver the appropriate ligand to the rest of the transporter (25).


**Figure 2. The PotABCD2D1 operon in *V. cholerae*.** This operon codes for the PotABCD2D1 transporter.

The PotABCD2D1 system (Figure 3) is thought to operate similar to the well-characterized PotABCD transport system in *Escherichia coli*, which is responsible for importing both spermidine and putrescine in to the cell. This system consists of PotA (an ATPase), PotB and PotC (channel forming proteins), and PotD (a substrate binding protein) (26, 27, 28). A closer analysis, using bioinformatics, of the *pot* gene cluster in *V. cholerae* suggested the role of each protein in the PotABCD2D1 operon coincided with the confirmed role within the *E. coli* system, albeit the *V. cholerae* system is hypothesized to have two substrate binding proteins as indicated by analysis of the operon using bioinformatics. In *E. coli*, all of the Pot proteins that are part of the transporter are essential for spermidine uptake (29) but in *V. cholerae* the PotD2 protein is not necessary for spermidine uptake (12). Little is known about polyamine uptake mechanisms in *V. cholerae*; therefore, a closer look at this system is warranted. Polyamine transport has been shown to affect other physiological responses of the cell. For example, *potD* gene expression in *Streptococcus pneumonia* has been shown to increase during infection and stressful environmental conditions implying that polyamines play a role in bacterial pathogenesis (16, 33). Deletion of the *potD1* gene in *V. cholerae* resulted in a loss of spermidine in the cell as well as an increase in biofilm formation. As *V.*

*cholerae* synthesizes only negligible amounts of spermidine under these conditions (24), this result suggested that PotD1 is responsible for the uptake of spermidine into the cell (12).

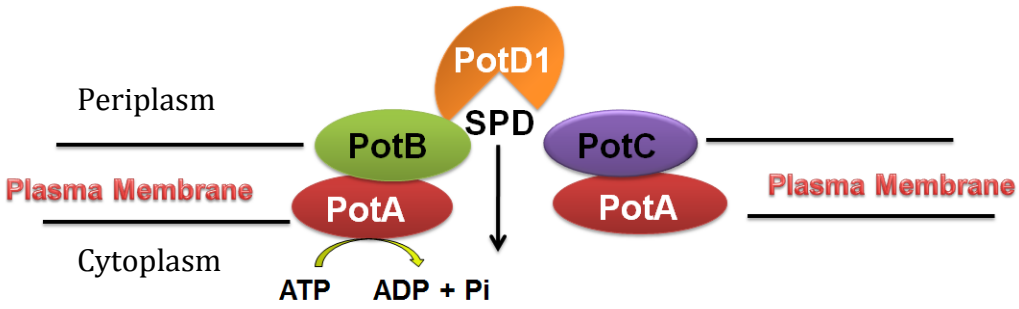


**Figure 3. Hypothesized cellular locations of the spermidine ABC transport system.** This system is encoded by the PotABCD2D1 operon in *V. cholerae*. SPD is the common polyamine spermidine.

Ubiquitous ABC transporters represent a diverse and often essential protein complex for cell survival. Substrate binding proteins, within an ABC transporter system, bind their substrates with affinities around 0.01 to 100 uM, and many can bind multiple ligands (30, 31, 32). Orthologs of the PotD1 protein are present among a diverse range of prokaryotic and archaeal species, illustrating the potential of similar function across many organisms (Figure 4), suggesting its importance in cellular functions as well as ancestral evolutionary presence.

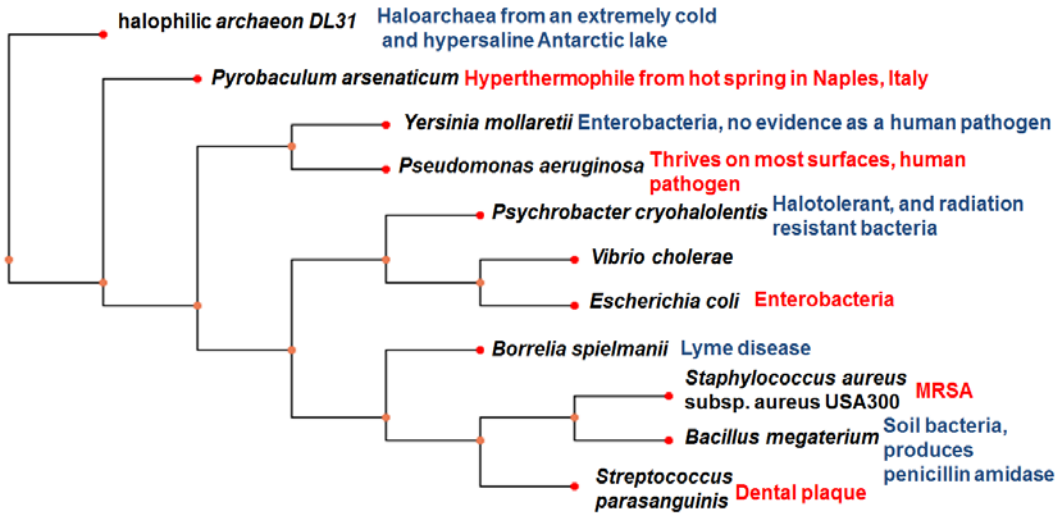


**Figure 4. Phylogenetic tree depicting PotD1 proteins from various prokaryotic species.** The tree is based upon the maximum parsimony method, Protpars, and drawn using PhyFi. ClustalW was used for multiple sequence alignment.

Because ABC transporters have a large impact on bacterial physiology, a greater understanding into mechanisms and abilities of ABC transporters is imperative. Understanding the mechanisms behind substrate specificity and binding interaction can prove useful in influencing protein function or in understanding protein interactions with therapeutic drugs. ABC transporters used for import can be especially good targets for drug development since they are generally unique to prokaryotes and are easily accessible due to their location in the periplasm of gram negative species or on the cell surface in gram positive species (34).

The purpose of this work was to more thoroughly characterize the binding properties of PotD1 to its ligands and ultimately its effect on biofilm formation in *V. cholerae*. This was done through genetic characterization of the ligand binding cleft and the protein's ability to interact with various polyamines which alter biofilm levels in this bacterium. Because spermidine and norspermidine differ by only one methylene group, I hypothesized that PotD1 may also interact with norspermidine. Therefore, the specific objectives of this

research included, i) to determine if PotD1 is able to bind norspermidine, ii) to compare binding affinities of spermidine and norspermidine to PotD1, iii) to determine the amino acid residues involved in the transport of spermidine by PotD1, and iv) to understand how biofilm formation is affected by increase or decrease in uptake activity of the PotD1 protein.

# MATERIALS AND METHODS

## *Bacterial strains, plasmids, media and reagents*

The bacterial strains, plasmids, and primers used throughout this study are listed in Table 1, Table 2, and Table 3, respectively. Primer synthesis and DNA sequencing were done by Eurofins MWG Operon (Huntsville, AL) and Cornell University (Ithaca, NY), respectively. All cell growth/cultures were done in Luria-Bertani broth (LB) (1% Tryptone, 0.5% Yeast Extract, 85 mM NaCl) unless otherwise stated. The polyamines were purchased from Sigma (St.Louis, MO). The restriction enzymes, *Xho*I, *Spe*I, *Eco*RI, *Nco*I, *Xmn*I, and *Phusion* and *OneTaq* polymerases were purchased from New England Biolabs (Beverly, MA). Chemicals were purchased from Sigma-Aldrich (St Louis, MI), Fisher Scientific (Fairlawn, NJ), or Amresco (Solon, OH) unless otherwise stated.

## *Deletion of the nspC gene*

To ensure that *V. cholerae* is not able to synthesize norspermidine, the carboxy-norspermidine synthesis gene (*nspC*) was deleted using double homologous recombination. The kanamycin aceytltransferase gene was amplified from pKD4 plasmid using the PA207 forward primer and PA208 reverse primer. A 371 base pair fragment upstream of the *nspC* gene was amplified using the primers P328 and P329. Similarly, a 468 base pair fragment downstream of the *nspC* gene was amplified using the P330 and P331 primers. The primers were designed such that the reverse primer, used for the amplification of the upstream *nspC*

fragment, contained complementary regions to PA207, and the forward primer, used for the amplification of the downstream fragment, contained complementary regions to PA208. The three PCR products were then spliced together by stitching by overlap extension PCR. After adding adenines, this product was cloned into a pCR2.1-TOPO vector following the manufacturer's instructions (Invitrogen, Carlsbad, CA), and the sequence was verified. This insert was then excised using *Xho*I and *Spe*I, and ligated into the pWM91 plasmid linearized with the same enzymes,[39] electroporated into electrocompetant SM10λpir *E. coli* using a BIO-RAD MicroPulser (Hercules, CA) at 1.8 kV, and verified using colony PCR. Single colonies were resuspended in 100 µl of water, heated at 95° C for 5 minutes, and used in colony PCR to screen colonies positive for the insert (2 µL of template DNA, 5 µL 5X *OneTaq* Standard Reaction Buffer, 200 µM dNTPs, 0.2 µM of each primer, and 0.125 µL *OneTaq* DNA polymerase in a 25 µL reaction). Cycling conditions were as follows: an initial denaturation at 94° C for 5 minutes, 30 cycles of 94° C for 30 seconds, 60° C for 30 seconds, 68° C for 60 seconds, and a final extension at 68° C for 5 minutes. This strain was used for exchange with wild-type *V. cholerae*. Fresh overnight plates for the recipient *V. cholerae* and donor *E. coli* containing the plasmid pWM91::Δ*npsC* (hereafter referred to as pAR17) were streaked on LB plates containing streptomycin (100 µg/mL) and ampicillin (100 µg/mL), respectively, and incubated overnight at 37° C. The next day, the donor pAR17 was mixed with recipient PW357 on LB agar plates and incubated at 37° C overnight. In the morning, half of the growth was streaked onto LB agar plates containing streptomycin (100 µg/mL) and ampicillin (50 µg/mL) agar for isolation and incubated at 37° C overnight. Four single colony isolates were streaked on LB agar containing kanamycin (30 µg/mL) and incubated at 37° C overnight. The next day, multiple colonies were picked and then streaked for isolation

on sucrose plates (10% Sucrose, 1% tryptone, 1.5% agar, 0.5% yeast) containing kanamycin (30 µg/mL), and streptomyocin (100 µg/mL). Colonies were also patched on LB agar containing ampicillin (50 µg/mL) and kanamycin (30 µg/mL) to ensure no growth and confirm successful homologous recombination.

***Extraction, benzoylation, and detection of polyamines***

To determine the identity and the levels of polyamines in *V. cholerae*, polyamines were extracted and analyzed as previously described (40, 12, 13). Briefly, all strains were grown at 27° C to mid-log phase, pelleted, washed with 1X Phosphate-buffered saline (137 mM NaCl, 2.7 mM KCl, 10 mM $Na_2HPO_4$, and 2 mM $KH_2PO_4$, pH 7.4), and resuspended in water at 10 µL per mg wet cell weight. Cells were then lysed using sonication, and debris was removed by centrifugation. The cellular protein was precipitated by a 50% Trichloroacetic acid solution (TCA) and centrifuged, leaving the supernatant containing the polyamines. This supernatant was removed and benzoylated. The benzoylation procedure as described previously (40, 12, 13) required extraction by 1 mL of chloroform twice. The sample was then evaporated to dryness, and dissolved in 100 µl mobile phase used for HPLC (60/40 ratio methanol and water). Along with the benzoylation of the samples, a standard mix containing 0.1 mM of each polyamine was prepared each time. HPLC utilized a Waters 1525 Binary Pump with a 2487 Dual Wavelength Absorbance Detector set at 254 nm and a Phenomenex Sphereclone 5u ODS column (5 µm, 250 X 4.6 mm) that was fitted with a 4.0 X 3.0 mm guard cartridge (Phenomenex, Torrance, CA). The runs were performed using a gradient of 45-60% methanol in water for 30 minutes with a 10 minute isocratic equilibration of 45% methanol in water. Per each run, 40 µl of each sample were injected into the column. To

understand if there is competition between norspermidine and spermidine uptake through the PotD1 protein, polyamines were added to the media in varying concentrations and cell extracts were analyzed as described previously.

***Construction of the potD1 gene variants using site-directed mutagenesis***

To further characterize the PotD1 protein, site-directed mutagenesis was used to alter the putative ligand binding site. The primers were designed to generate five different mutations in the PotD1 protein, namely, W32L, W252L, E168A, D254N, and D254A. *Phusion* polymerase was used to amplify the *potd1* gene in two fragments: the upstream piece was amplified using a forward primer that annealed at the beginning of the *potd1* gene sequence and a reverse mutagenic primer, and a forward mutagenic primer and a reverse primer were used for the downstream piece. The mutagenic primers were complementary which allowed splicing together of the pieces using overlap extension PCR. The PCR products were separated on a 1% agarose gel and purified using the GE Healthcare Illustra GFX PCR DNA and Gel Band Purification Kit (Buckinghamshire, UK). The reverse primer, PA144, encoded a V5 epitope tag which allowed incorporation of this antigenic tag into each mutant. Pieces were spliced together by overlap extension PCR in a reaction volume of 50 µL with 0.5 µM of each primer (PA138 and PA144), 200 µM dNTPs, 10 µL of 5X Phusion HF Buffer, 0.5 µL *Phusion* Polymerase, and 10 µL of each PCR product. Cycling parameters were as follows: an initial denaturation at 98° C for 30 seconds, 30 cycles of denaturation at 98° C for 10 seconds, annealing at 60° C for 30 seconds, extension at 72° C for 30 seconds, and a final extension at 72° C for 5 minutes. The correct size product was excised from the gel, purified, and adenines were added to the blunt ended PCR products using *OneTaq* polymerase by

incubation at 72° C for 10 minutes. The mutated genes were cloned into a pCR2.1-TOPO vector (Invitrogen, Carlsbad, CA) and electroporated into electrocompetant DH5α cells using a BIO-RAD MicroPulser (Hercules, CA) at 1.8 kV. The transformed cells were incubated in SOC medium at 37° C for 1 hour at 200 rpm, and then plated on LB-ampicillin (100 ug/mL) with 40 µl of X-gal (20 mg/mL in dimethylformamide). Blue-white screening was used for selection of white or light blue colonies, indicative of plasmids carrying the insert. Colony PCR, as described previously, was used to confirm the presence of the insert. Colonies positive for the insert were grown overnight, plasmids were purified using the Promega Wizard Plus SV Minipreps DNA Purification System (Madison, WI) and sequenced to confirm the presence of the mutations. The inserts were excised from this plasmid using *Eco*RI and *Nco*I, ligated into a *V. cholerae* compatible pACYC184 plasmid linearized with the same enzymes, and transformed into DH5α cells. These colonies were screened again for the insert using colony PCR as described above; colonies positive for the insert were grown overnight, plasmids were purified and transformed into a *V. cholerae potD1* mutant and a Δ*potD1*Δ*nspC* double mutant.

***Western Blotting to confirm the presence of mutant PotD1 proteins***

Cells were grown overnight in LB broth, pelleted, resuspended in water, and lysed using Novagen BugBuster reagent following the manufacturer's instructions (Darmstadt, Germany). Samples were loaded on a denaturing gel with a 12% acrylamide resolving gel and 5% stacking gel and run at 250 V for 1 hour. The gel and blotting paper were equilibrated in 1X Transfer Buffer containing 50 mM TRIS, 40 mM Glycine, and 1.5 mM SDS. A PVDF membrane was quickly exposed to methanol and then incubated in 1X

transfer buffer. The gel was transferred to the membrane using a BIO-RAD TransBlot (Hercules, CA) for 15 minutes at 15 V. The membrane was blocked overnight with 3% skim milk in 1X PBS (137 mM NaCl, 2.7 mM KCl, 10 mM $Na_2HPO_4$, and 2 mM $KH_2PO_4$, pH 7.4) at 4° C, and incubated with the V5 antibody conjugated to HRP (AbD Serotec, Raleigh, NC), as a 1:1,000 dilution in a 3% skim milk in PBS, for 1 hour with the membrane at room temperature. The membrane was then washed three times in PBS with 0.05% Tween 20 and visualized calorimetrically using 1-Step TMB-Blotting HRP membrane substrate (Thermo Scientific, Rockford, IL). Alternatively, the antibody dilution was adjusted and the membrane was incubated with SuperSignal West Pico or Femto Chemiluminescent Substrate (Thermo Scientific) for 5 minutes. The membrane was exposed to X-ray film (Bioexpress, Kaysville, UT) and developed using a Konica Minolta SRX-101A developer (Konica Minolta Medical & Graphic, Inc., China).

***Sequence Analysis***

The sequence of the PotD1 protein (VchoM_00690.1) of *V. cholerae* O139 was obtained from the *V. cholerae* sequence database maintained at the Broad Institute (Cambridge, MA). A protein Blast search was performed on the NCBI database, using the PotD1 sequence, with default parameters, to find homologs of this protein in the database. Using multiple sequence alignment (MSA), the PotD1 protein was aligned with the *E. coli* PotD protein. Briefly, the sequences were retrieved using the fasta format and were saved in a text program with a fasta extension. This file was used for MSA on the ClustalW alignment website (http://www.ebi.ac.uk/Tools/msa/clustalw2/). The alignment files were saved in phylip format.

### *Maximum parsimony to determine phylogeny*

A maximum parsimony phylogenetic tree was generated using phylip. The ClustalW file with phylip extension was loaded into the protpars server, which can be found at the Mobyle @ Pasteur website (http://mobyle.pasteur.fr/cgi-bin/portal.py#forms::protpars). The outgroup species was adjusted to an archaea species. The propars tree file was then saved and uploaded into the Phyfi tree drawing program (http://cgi-www.daimi.au.dk/cgi-chili/phyfi/go).

### *Modeling of the PotD1 and PotD2 protein*

SWISS-MODEL was used to predict protein structure using homology to crystal structures in the Protein Data Bank (http://www.rcsb.org/pdb/home/home.do). The automated protein structure depiction tool was used. The PotD1 protein sequence was uploaded and a characterized homologous protein structure was used as the template to configure the hypothesized structure. The results were analyzed via the SWISS MODEL server once complete, and the pdb file was downloaded for further manipulation. The MOLSOFT ICM Browser was used to view the pdb files, give secondary structure prediction, and manipulate the structure.

***Biofilm assays***

Biofilm assays as previously described (41) were performed in triplicate with all mutants multiple times. Briefly, strains were inoculated from overnight cultures and grown at 27° C for 24-48 hours, planktonic cells were harvested, and glass beads were used to collect the biofilm. A microplate reader (Bio-Rad, Hercules, CA) using a 655 nm filter was used to quantify planktonic and biofilm cell density.

***pMAL-p5X fusion constructs for protein expression***

The pMAL Protein Fusion and Purification System (New England Biolabs, Ipswich, MA) was used to construct the recombinant PotD1 protein. Briefly, the *potD1* gene was amplified, using primers PA193 and PA194 with *Phusion* polymerase, without its signal sequence as predicted by SignalP 4.0 (http://www.cbs.dtu.dk/services/SignalP/). An *Nco*I restriction site was engineered into PA194 for cloning into the pMAL-p5X vector in frame with a gene encoding the maltose binding protein. The *potD1* gene was restricted using *Nco*I and leaving a blunt end on the 3' end of the PCR product, purified using the GE Healthcare illustra PCR and DNA Purification Kit, ligated into the pMAL-p5X vector linearized using *Xmn*I (a blunt end cutter) and *Nco*I, and transformed into NEB Express *E. coli* (NEB). The presence of the insert was confirmed using colony PCR and plasmids from colonies containing the positive clones were isolated and sequenced to confirm no errors were present in the sequence.

***Purification of MBP-PotD1 fusion protein***

The pMAL manual for extracting the periplasm was followed with minor changes. One liter of M9 minimal media (0.6 % $Na_2HPO_4$, 0.3 % $KH_2PO_4$, 0.05 % NaCl, 0.1 % $NH_4Cl$,

0.2 % glucose, 1 mL 1M $MgSO_4$, 1 mL 0.1M CaCl, and a final concentration of 0.15% cassamino acids) with ampicillin (100 µg/mL) was inoculated with a 20 mL overnight of cells in the same medium and grown 5 hours at 37° C at 220 rpm. Isopropyl β-D-1-thiogalactopyranoside (IPTG) was then added to a final concentration 0.3 mM and incubated at 30° C for 3 hours. The cells were harvested at 4000 x g for 20 minutes and the supernatant was discarded. Cells were resuspended in 80 mL per gram of wet cell weight in 30 mM Tris-HCl, 20% sucrose, pH 8.0. Ethylenediaminetetraacetic acid (EDTA) was added to 1 mM and incubated 10 minutes at room temperature with shaking. The cells were centrifuged at 8000 x g for 20 minutes at 4° C, the supernatant was removed, and the pellet was resuspended in the same amount of ice-cold 5 mM $MgSO_4$ and shaken for 10 minutes in an ice-bath. The cells were centrifuged at 8000 x g for 20 minutes at 4° C, and the supernatant, which contained the periplasmic fraction, was collected. To the supernatant, 8 mL of 1 M Tris-HCl (pH7.4) and 0.1 M phenylmethanesulfonylfluoride (PMSF) final concentration was added. Four mL of amylose resin was equilibrated with column buffer (20 mM Tris, 200 mM NaCl, and 1 mM EDTA) and added to the supernatant for incubation overnight at 4°C. The slurry was then centrifuged at 4700 x g for 10 minutes multiple times to collect the resin into one conical tube. The resin was then loaded on a column and washed with 12 mL of column buffer. The protein was eluted with 10 mL column buffer containing 10 mM maltose. One mL fractions were collected, fractions containing protein were determined using a Bradford assay, and visualized using SDS-PAGE. These fractions were pooled and concentrated to 1 mg/mL, and stored with 50% glycerol at -20° C.

Table 1. **Bacterial strains.**

| Strains | Genotype | Reference/source |
|---|---|---|
| ***E. coli*** | | |
| DH5α | F-φ80*lacZ*ΔM15, Δ(*lac*ZYA-*argF*)U169, *deoR*,*recA*1, *phoA*, *endA*1, *hsd*R17(*rk*2, *mk*+), *supE*44, *thi*-1, *gyrA*96, *re/A*1, λ- | Invitrogen |
| SM10λpir | thi thr leu tonA lacY supE recA<RP4-2-Tc<MulpirR6K; | Miller & Mekalanos (1988) [57] |
| NEB Express | Kmr *fhuA2 [Ion] ompT gal sulA11 2 R(mcr-73::miniTn10—TetS) [dcm] R(zgb-210::Tn10—TetS) endA1 Δ(mcrC-mrr)114::IS10* | New England Biolabs |
| ***V. cholerae*** | | |
| PW249 | MO10, clinical isolate of V. cholerae O139 from India $Sm^R$ | Waldor & Mekalanos (1994) [58] |
| PW357 | MO10*lacZ*::*vpsLp* → lacZ, $Sm^R$ | Haugo & Watnick (2002) [59] |
| AK059 | MO10Δ*potD1*, $Sm^R$ | McGinnis *et al*. (2009) [12] |
| AK160 | PW357Δ*potD1*, $Sm^R$ | This study |
| AK164 | PW357Δ*potD1* w/ pACYC184, $Tet^R$ | This study |
| AK103 | MO10 w/ pACYC184 | This study |
| AK314 | PW357Δ*nspC*, $Sm^R$ | This study |
| AK317 | PW357Δ*potD1*Δ*nspC*, $Sm^R$ | This study |
| AK165 | MO10Δ*potD1* w/ pAR2 | This study |
| AK214 | MO10Δ*potD1* w/ pAR6 | This study |
| AK268A | MO10Δ*potD1* w/ pAR13 | This study |
| AK205 | MO10Δ*potD1* w/ pAR8 | This study |
| AK213 | MO10Δ*potD1* w/ pAR7 | This study |
| AK266B | MO10Δ*potD1* w/ pAR11 | This study |
| AK330 | PW357Δ*potD1*Δ*nspC* W/ pAR6 | This study |
| AK331 | PW357Δ*potD1*Δ*nspC* w/ pAR7 | This study |
| AK332 | PW357Δ*potD1*Δ*nspC* w/ pAR11 | This study |
| AK326 | PW357Δ*potD1*Δ*nspC* w/ pAR8 | This study |
| AK327 | PW357Δ*potD1*Δ*nspC* w/ pAR13 | This study |
| AK333 | PW357Δ*potD1*Δ*nspC* w/ pAR2 | This study |

Table 2. **Bacterial plasmids.**

| Plasmids | Genotype | Reference/source |
|---|---|---|
| pCR2.1-TOPO | TOPO cloning plasmid, $Ap^R$ | Invitrogen |
| pACYC184 | cloning plasmid, low copy, $Tet^R$ | New England Biolabs |
| pGEM-T | pGEM-T easy cloning vector, $Ap^R$ | Promega |
| PWM91 | *oriR*6k, *lacZα*, *sacB*, homologous recombination plasmid, $Ap^R$ | Metcalf et al. (1996) [39] |
| pKD4 | template plasmid, $Ap^R$, $Kan^R$ | Datsenko & Wanner (2000) [60] |
| pMAL-p5X | protein expression plasmid, $Ap^R$ | New England Biolabs |
| pAR1 | pGEMT::*potD1V5* | This study |
| pAR2 | pACYC184::*potD1V5* | This study |
| pAR6 | pACYC184::*potD1* (E168A) | This study |
| pAR7 | pACYC184::*potD1* (W252L) | This study |
| pAR8 | pACYC184::*potD1* (D254N) | This study |
| pAR11 | pACYC184::*potD1* (D254A) | This study |
| pAR13 | pACYC184::*potD1* (W32L) | This study |
| pAR14 | pMAL-p2X:: *potD1* | This study |
| pAR18 | pMAL-p2X:: *potD1* (W252L) | This study |
| pAR17 | pWM91::Kan cassette w/ flanking nspC regions | This study |

Table 3. **Primers.**

| Primer | Description | Sequence |
|---|---|---|
| PA138 | Forward primer for the *potD1* gene | 5'- ACGCCTAGTTAGGTTCTTTC-3' |
| PA144 | Reverse primer for the *potD1* gene with a V5 tag | 5'CCATGGCTACGTAGAATCGAGACCGAGGA AGGGTTAGGGATAGGCTTACCGCCGCTGC CGCT GCCATCGTTCACTTTTAGCTTTTGG-3 |
| PA182 | Reverse primer for the *potD1* gene | 5'- CCATGGCTACGTAGAATCG-3' |
| PA167 | W32L mutant forward primer | 5'-CTTTATTTCTACAACCTGTCTGAATATATC-3' |
| PA168 | W32L mutant reverse primer | 5'-GATATATTCAGACAGGTTGTAGAAATAAAG-3' |
| PA169 | E168Q mutant forward primer | 5'-GATGACGCTCGTCAAGTCTTCCATATC-3' |
| PA170 | E168Q mutant reverse primer | 5'-GATATGGAAGACTTGACGAGCGTCATC-3' |
| PA171 | E168A mutant forward primer | 5'-GATGACGCTCGTGCAGTCTTCCATATC-3' |
| PA172 | E168A mutant reverse primer | 5'-GATATGGAAGACTGCACGAGCGTCATC-3' |
| PA173 | W252L mutant forward primer | 5'-CACCATTTTTCTGATGGACAGCATC-3' |
| PA174 | W252L mutant reverse primer | 5'-AGTGCTGTCCATCAGAAAAATGGTG-3' |
| PA175 | D254N mutant forward primer | 5'-CATTTTTTGGATGAACAGCATCTCGATTC-3' |
| PA176 | D254N mutant reverse primer | 5'-GAATCGAGATGCTGTTCATCCAAAAAATG-3' |
| PA177 | D254A mutant forward primer | 5'-CATTTTTTGGATGGCCAGCATCTCGATTC-3' |
| PA178 | D254A mutant reverse primer | 5'-GAATCGAGATGCTGGCCATCCAAAAAATG-3' |
| PA193 | pMalp2X PotD1 forward primer | 5'-AAAGACCAAGAACTTTATTTCTAC-3' |
| PA194 | pMalp2X PotD1 reverse primer | 5'-CGCCCATGGTTAATCGTTCACTTTTAGC-3' |
| PA207 | *NspC* deletion pKD4 amplification forward primer | 5'TGCGGCCGCTCGTAACAA GAGACAGGATGAGGATC-3' |
| PA208 | *NspC* deletion pKD4 Reverse primer | 5'-TTACGAGCGGCCGCATCA GAAGAACTCGTCAAGAAG-3' |
| P328 | Upstream *nspC* deletion forward primer | 5'-GTGTATTCAATATGGAGCAGC-3' |
| P329 | Upstream *nspC* deletion reverse soe primer | 5'-TTACGAGCGGCCGCACA TGAAGTATGGGGTTCTC-3' |
| P330 | Downstream *nspC* deletion forward soe primer | 5'-TGCGGCCGCTCGTAAAATGGC CTGAAAATGCCGTCG-3' |
| P331 | Downstream *nspC* deletion reverse primer | 5'-TCTAAGCAGCGTTCAGAAGC-3' |

# RESULTS

## *Construction of a V. cholerae mutant unable to synthesize norspermidine*

Because *V. cholerae* is able to synthesize norspermidine, I first constructed a strain unable to synthesize this molecule in order to assess norspermidine import. Multiple attempts to delete the *nspC* gene in *V. cholerae*, to ensure that *V. cholerae* could not synthesize norspermidine, have been unsuccessful. For example, an attempt was made to replace the *nspC* gene with a markerless in-frame deletion which failed (42). In addition, I attempted to use ʎ-Red phage recombineering to delete this gene with no success. These initial failures suggested that the deletion of the *nspC* gene may affect cell health; therefore, we decided to use a positive selection system utilizing an antibiotic resistance gene. Homologous recombination using SacB counter-selectable mutagenesis was used to delete the *nspC* gene, but only with the addition of an antibiotic selection marker (Figure 5).

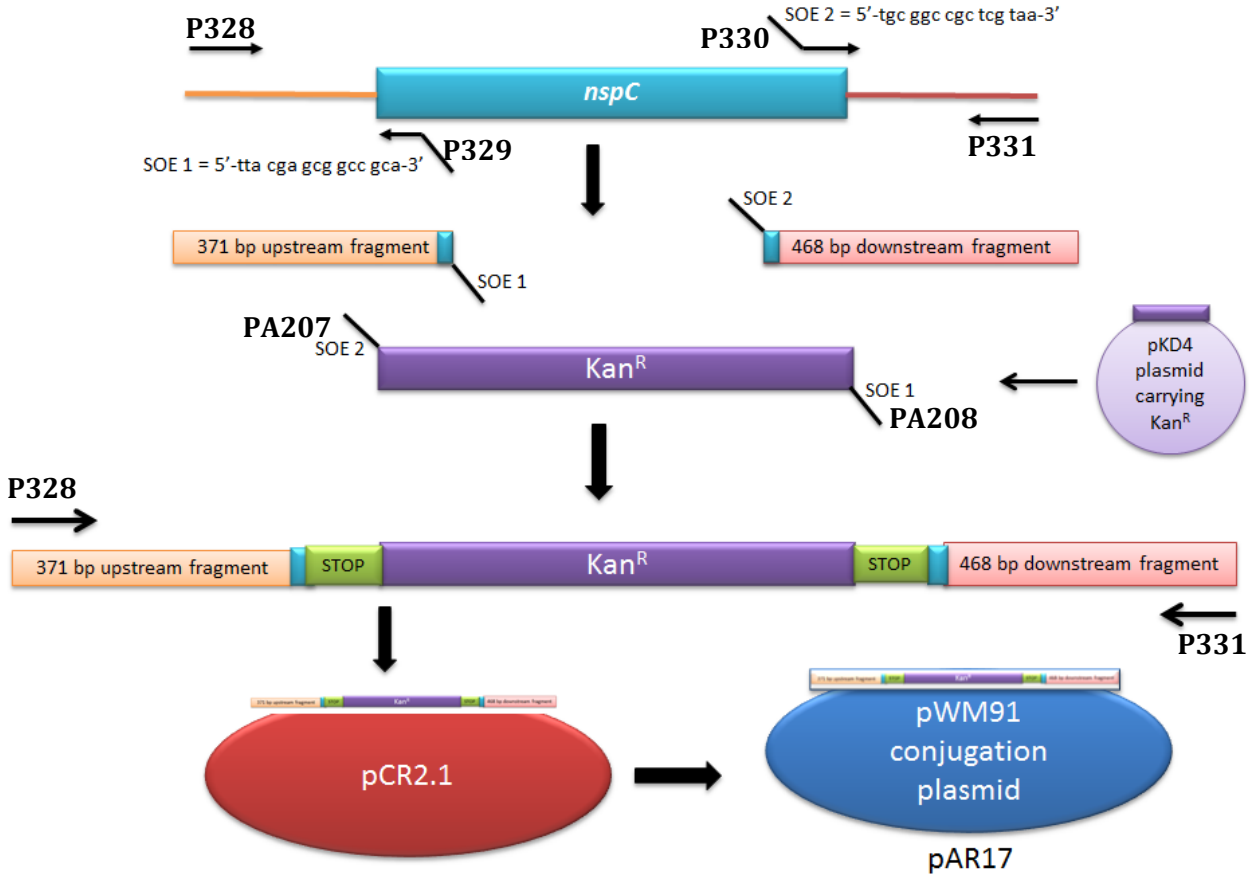


**Figure 5. Scheme representing the construction of the pAR17.** The pAR17 conjugation plasmid was used to replace the *nspC* gene in *V. cholerae* with a kanamycin resistance marker. The primer sequences are listed in Table 3. SOE presence indicates complementary regions.

First, a linear construct missing the *nspC* gene and containing the kanamycin acetyltransferase cassette was constructed. A region upstream of the *nspC* gene was amplified using P328 and P329, resulting in a 338 bp fragment, lane 3 on figure 6. A region downstream of the *nspC* gene was amplified using P330 and P331, resulting in a 468 bp fragment, lane 6 figure 6. In order to splice the three pieces using overlap extension PCR (SOE), primers P329 and P330 were engineered with SOE tags which were complementary to the SOE tags on the primers, PA207 and PA208, used for amplification of the 822 bp kanamycin acetyltransferase cassette from the pKD4 plasmid, lane 4 figure 6 (Figure 6). This allowed the upstream and downstream fragments to be spliced to the kanamycin

acetyltransferase cassette using the outside P328 and P331 primers, resulting in a 1780 bp fragment, lane 3 figure 7 (Figure 7). In this construct, the majority of the *nspC* coding sequence has been removed and replaced by the kanamycin acetyltransferase cassette. Adenines were added and this insert was cloned into a pCR2.1 TOPO plasmid, making use of the thymine overhangs using manufacturer's instructions, and verified using colony PCR with the M13 forward and reverse primers (Figure 8). After verification of the sequence, one plasmid isolated from a clone was digested and inserted into a linearized pWM91 plasmid (Figure 9), resulting in the pAR17 conjugation plasmid. Presence of the insert was confirmed using colony PCR (Figure 10) and this plasmid was mobilized into *V. cholerae* wild-type cells using homologous recombination with SacB counterselectable mutagenesis as described in the methods. The kanamycin and streptomycin resistant, ampicillin sensitive colonies were used to confirm the presence of the Δ*nspC*::*kan* construct by colony PCR (Figure 11).

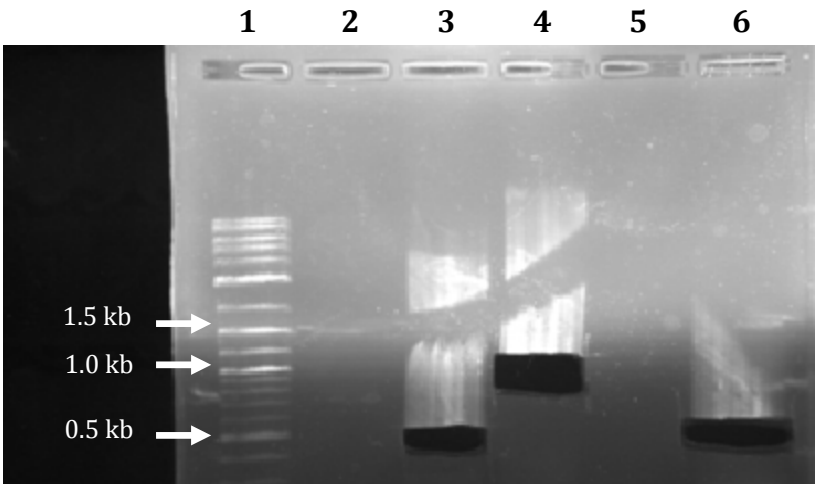


**Figure 6. A gel electrophoresis of pAR17 fragment excision.** This image depicts the 3 separate fragments used for construction of the linear segment of DNA containing the *Kan*$^R$ cassette. The lanes are as follows: lane 1 is the 2-log ladder, lane 3 is the upstream 338 bp fragment, lane 4 is the 822 bp Kan$^R$ cassette, lane 6 is the downstream 468 bp fragment, and lanes 2 and 5 are empty. The black boxes indicate excised fragments.

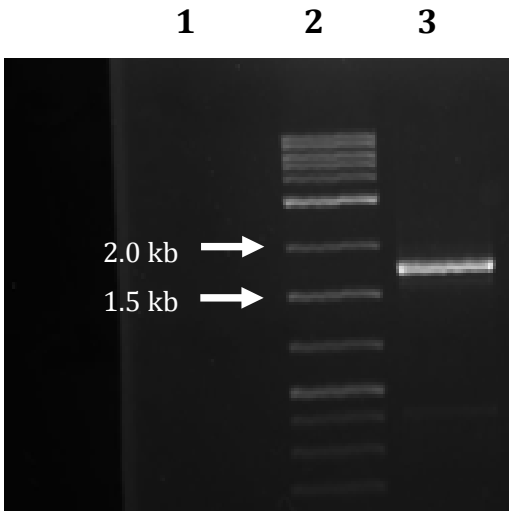


**Figure 7. Gel electrophoresis of the pAR17 fused product.** This image represents the fused product of both upstream and downstream pieces with the *Kan*$^{R}$ cassette**.** Lane 2 represents the 2-log ladder and lane 3 indicates the fused product at 1780bp.

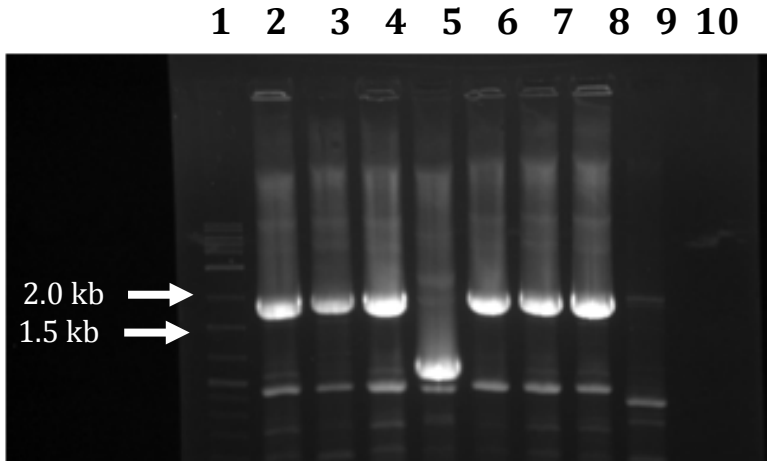


**Figure 8. Colony PCR of Δ*npsC*::*kan*.** Lane 1 is the 2-log ladder, lanes 2-9 are individual colonies and the brightest band is representative of the 1781 bp band. Lane 2 was chosen for further manipulation.

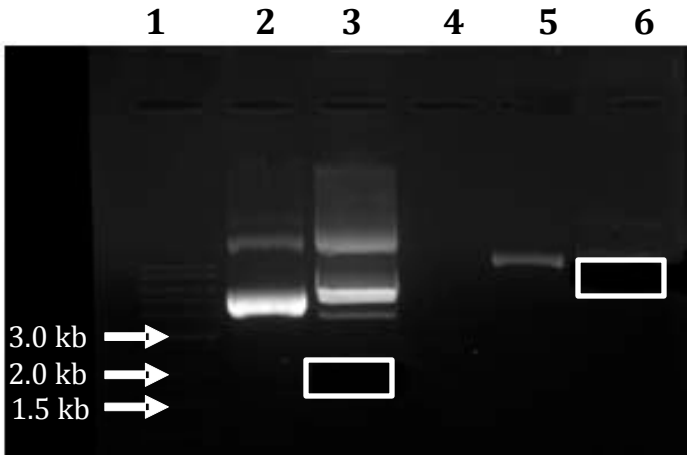


**Figure 9. Gel electrophoresis of the undigested and digested plasmids.** The lanes are as follows: lane 1 is the 2-log ladder, lane 2 the undigested Δ*nspC*::*kan* linear construct in the plasmid vector, lane 3 the digested Δ*nspC*::*kan* linear construct, lane 4 is empty, lane 5 is pWM91 undigested plasmid, and lane 6 is pWM91 digested plasmid. The black boxes indicate excised fragments.

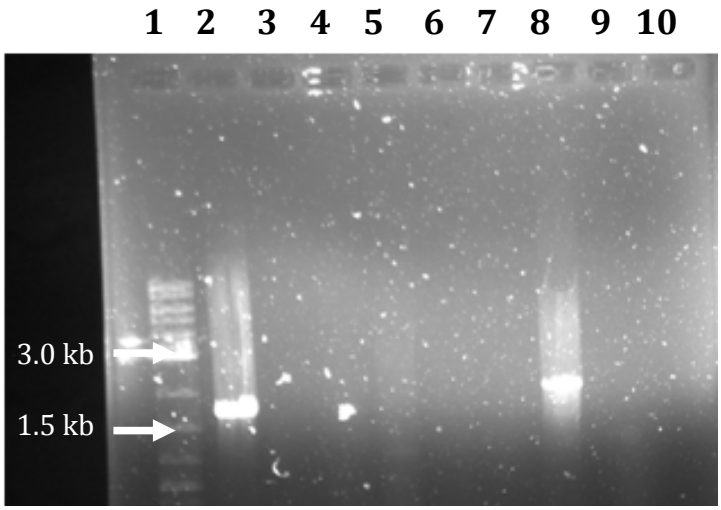


**Figure 10. Colony PCR of Δ*npsC*::*kan* in the pWM91 vector.** Lane 1 represents the 2-log ladder, lane 2 is a colony positive for the insert, lanes 3-7 are colonies in which the insert was not present or did not amplify. Lane 8 represents wild-type *V. cholerae nspC* amplification. Lane 9 and 10 are empty. The primers used were P331 and P328.

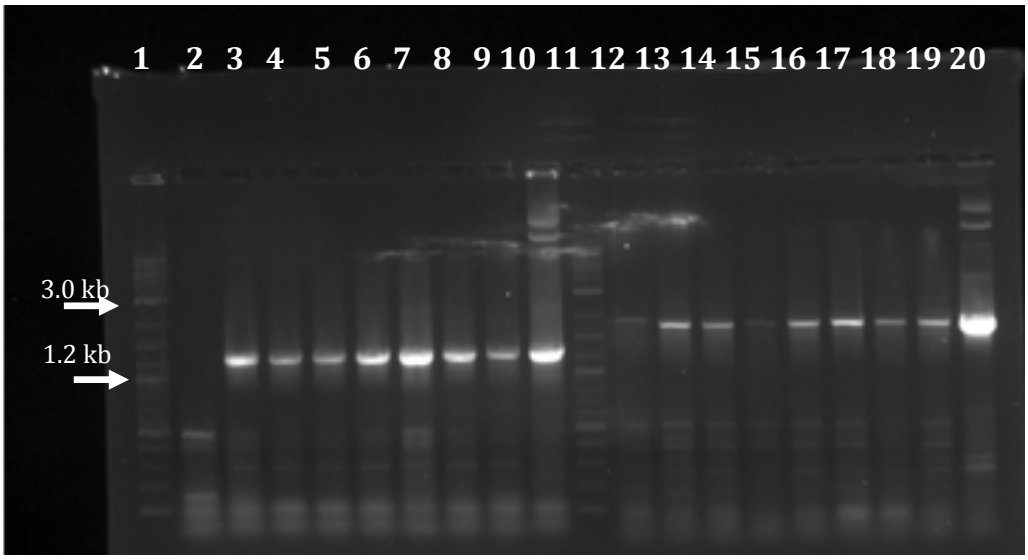


**Figure 11. Colony PCR confirmation of *nspC* deletion.** This gel is representative of the same colonies under two different conditions. The first and eleventh lane represent the 2-log ladder. Lanes 3-10 are the colonies amplified with P328 and P208 resulting in a 1312 bp band, used as a control to indicate colony amplification was possible. Lanes 13-20 are identical colonies amplified with the P328 and P331 primers resulting in a 1780 bp band. Lanes 2 and 12 are a wild-type *V. cholerae* and the *nspC* gene is amplified in lane 12 with a 1787 bp band.

### *Confirmation of the lack of norspermidine present in V. cholerae ΔnspC*

To confirm the Δ*nspC*::*kan* mutant was deficient in synthesizing norspermidine, high performance liquid chromatography (HPLC) was used to determine the polyamine levels present in the cells. A standard polyamine mix containing putrescine, diaminopropane, cadaverine, norspermidine, and spermidine, respectively, were quantified (Figure 12A) and peak retention times were compared to the wild-type *V. cholerae* (Figure 12B) and *V. cholerae* Δ*nspC* mutant (Figure 12C). The Δ*nspC* mutant was deficient in its ability to synthesize norspermidine, confirming the deletion of the *nspC* gene.

**A**

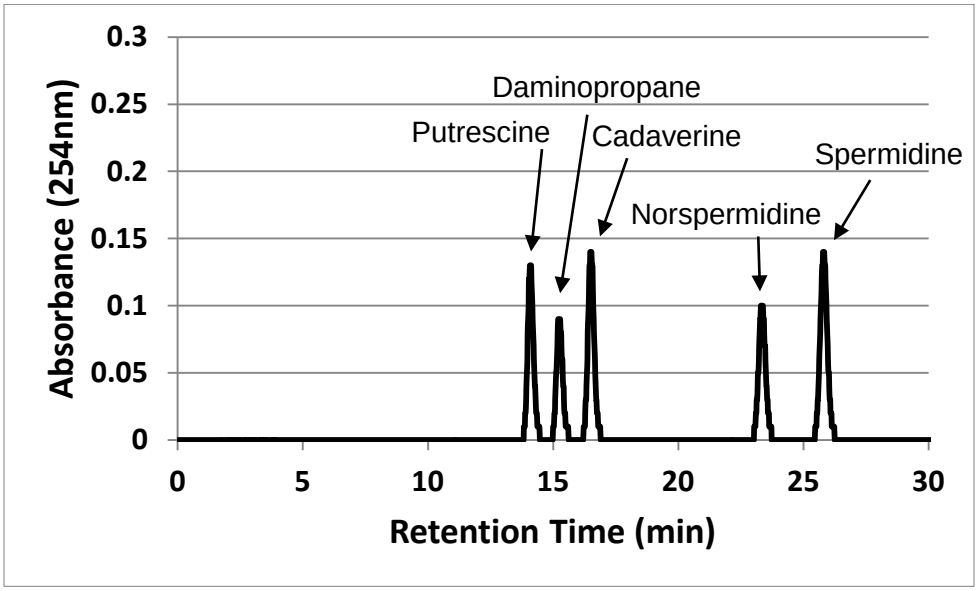
Absorbance (254nm)
0.3
0.25
0.2
0.15
0.1
0.05
0
0
5
10
15
20
25
30
Retention Time (min)
Daminopropane
Putrescine
Cadaverine
Spermidine
Norspermidine

**B.**

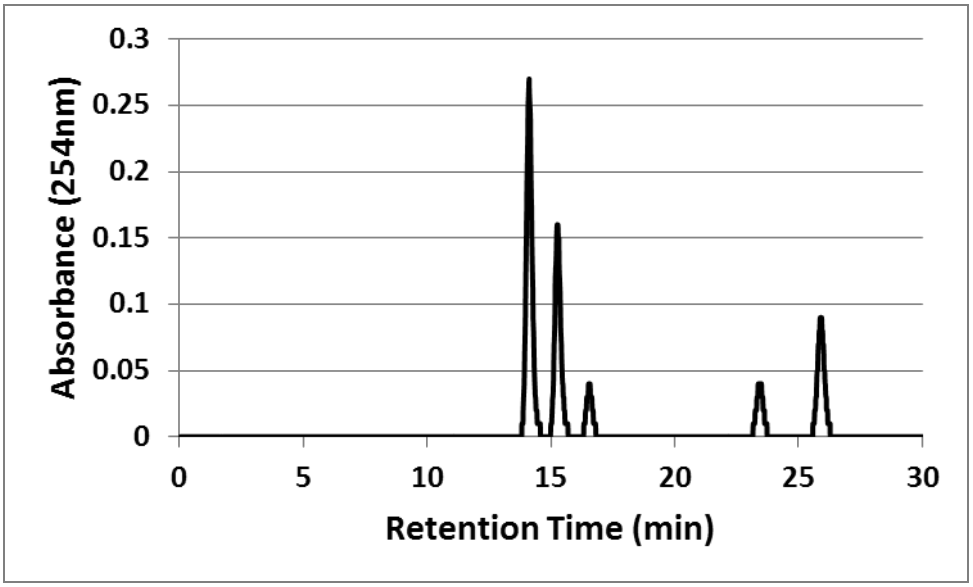
Absorbance (254nm)
0.3
0.25
0.2
0.15
0.1
0.05
0
0
5
10
15
20
25
30
Retention Time (min)

**C.**

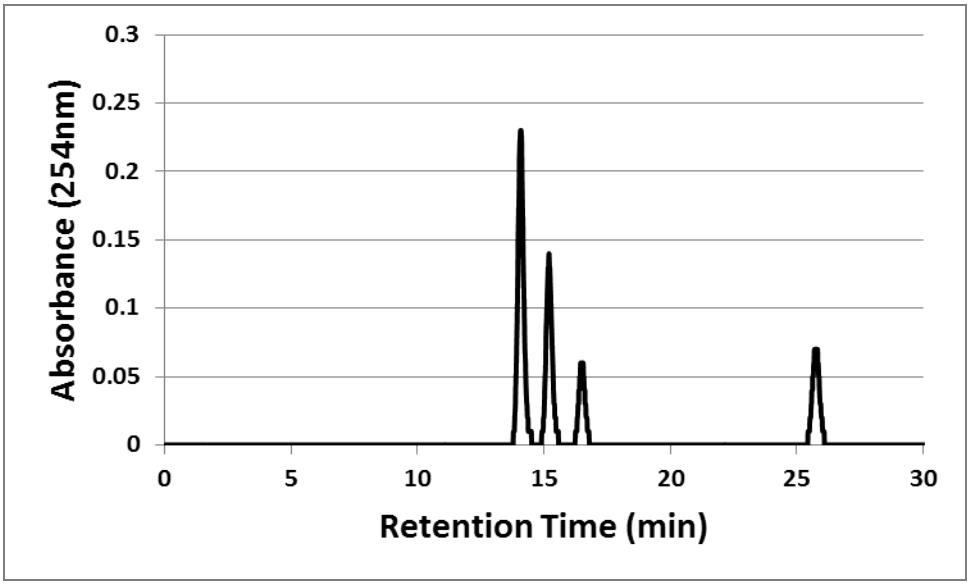


**Figure 12. Confirmation of a lack of norspermidine using HPLC. A)** HPLC chromatogram depicting the retention times of each polyamine. The peaks are representative of putrescine, diaminopropane, cadaverine, norspermidine, and spermidine, respectively. **B)** HPLC chromatogram representing wild-type *V. cholerae*. **C)** HPLC chromatogram confirming a lack of norspermidine in the *V. cholerae* Δ*nspC* mutant.

***Identification of a norspermidine transporter***

In order to assess the ability of PotD1 to act as a norspermidine transporter, first a double mutant was constructed. Homologous recombination was used to delete the *potD1* gene from the *V. cholerae* Δ*nspC* mutant in the same manner as previously stated. Because *V. cholerae* cannot synthesize much spermidine under these conditions, the cellular spermidine results from the import of spermidine in the media. Therefore, a Δ*nspC*Δ*potD1* double mutant should not contain any spermidine or norspermidine. This hypothesis was explored through the quantification of intracellular polyamines using HPLC, as previously stated, and it was confirmed that no spermidine or norspermidine was present in this mutant (Figure 13).

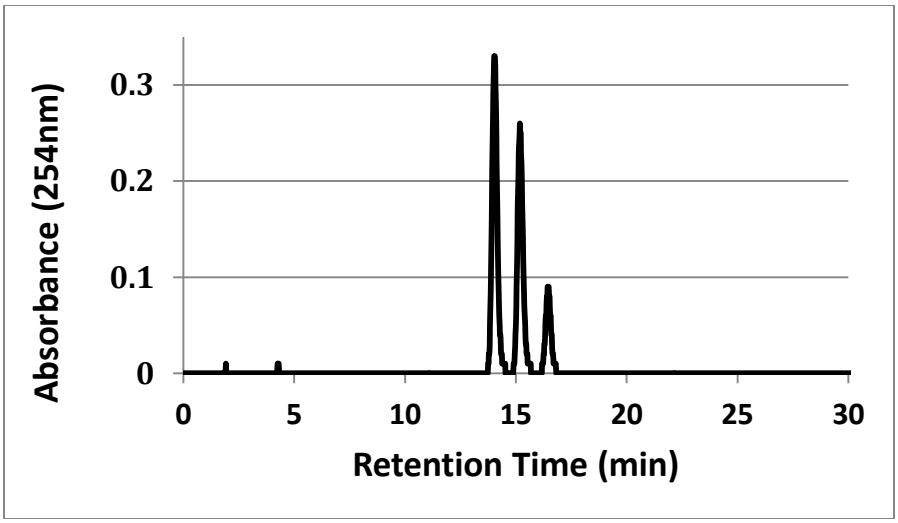


**Figure 13. Polyamines present in the *V. cholerae* Δ*nspC* Δ*potd1* mutant using HPLC.** The polyamines present are putrescine, diaminopropane, and cadaverine, respectively.

The polyamine retention times were compared to the standard polyamine retention times (Figure 12A). Upon confirmation of the inability of the *V. cholerae* Δ*nspC* Δ*potd1* mutant to uptake spermidine, the potential of PotD1 to act as a norspermidine transporter was explored. The *V. cholerae* Δ*nspC* strain containing the wild-type PotD1 protein was used to determine the ability of this protein to transport norspermidine. With the addition of 1 mM norspermidine to the media, a norspermidine peak was confirmed and the spermidine peak was no longer present (Figure 14). These results were also previously seen in wild-type *V. cholerae,* with the addition of 1mM norspermidine to the media, suggesting spermidine import is being blocked through PotD1 in the presence of norspermidine. To ensure that norspermidine was imported into the cell by PotD1 and not by a different low affinity transporter, polyamines in a Δ*npsC*Δ*potD1* mutant grown in the presence of 1 mM norspermidine were quantified. This mutant was not able to import norspermidine, indicating that PotD1 is responsible for norspermidine import (Figure 15). These results established the role of PotD1 to act as a substrate binding protein to both spermidine and norspermidine.

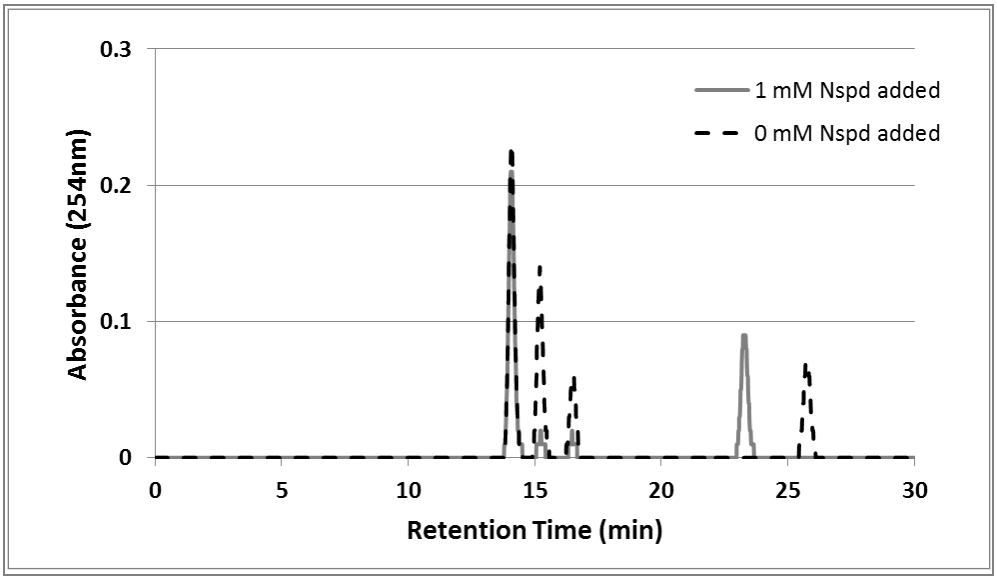


**Figure 14. *V. cholerae* Δ*nspC* mutant with 0 mM Nspd and with 1 mM Nspd.** Norspermidine is represented as Nspd. The dashed line represents 0 mM Nspd. The gray line represents 1 mM Nspd.

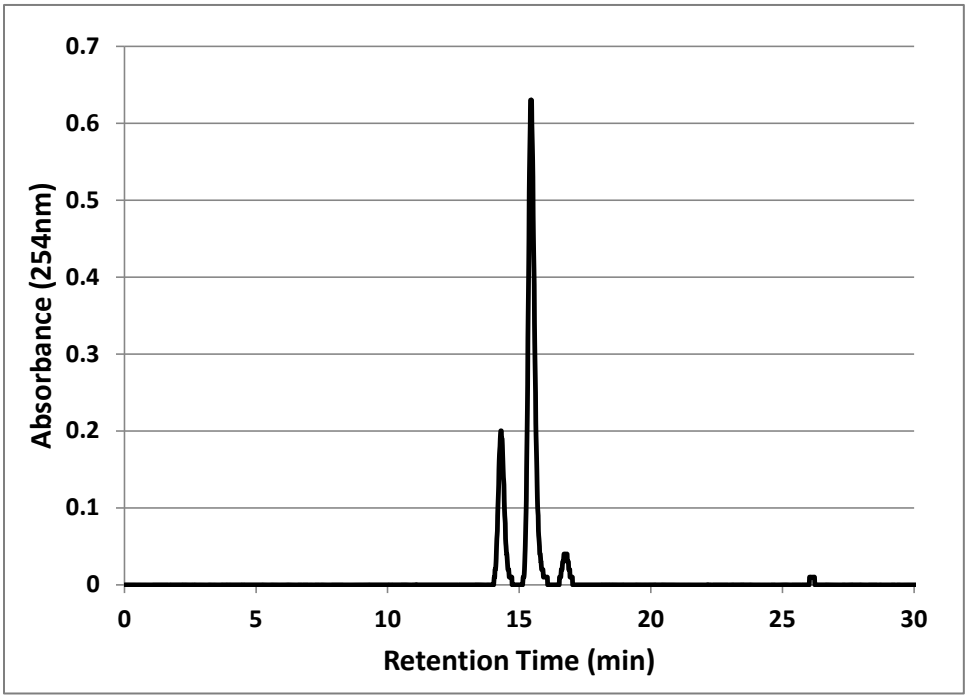


**Figure 15. *V. cholerae* Δ*nspC Δpotd1*mutant with 1 mM Nspd.** The peaks present are putrescine, diaminopropane, and cadaverine, respectively.

***PotD1 preferentially binds spermidine over norspermidine***

In order to assess the affinity of PotD1 for spermidine and norspermidine, competition assays were performed. The *V. cholerae* Δ*nspC* strain was grown with varying amounts of norspermidine added exogenously. The exogenous spermidine present in the LB media was quantified by benzoylation and HPLC. It was determined that spermidine was present at 10 +/- 13 uM in the environment (Figure 16 D), and the addition of 1 uM, 100 uM, and 1 mM exogenous norspermidine allowed for the characterization of PotD1 affinity for norspermidine and spermidine (Figure 16 A and B). Addition of 1 and 100 uM of norspermidine did not result in uptake of norspermidine, suggesting that PotD1 has a substantially higher affinity for spermidine than norspermidine (Figure 16 A and B). Norspermidine uptake occurred only upon the addition of 1 mM norspermidine, which is approximately 100 fold in excess to spermidine (Figure 16 C). These results show spermidine has a higher binding affinity to PotD1 than norspermidine, indicating that spermidine is the preferred ligand for the PotABCD1 transporter.

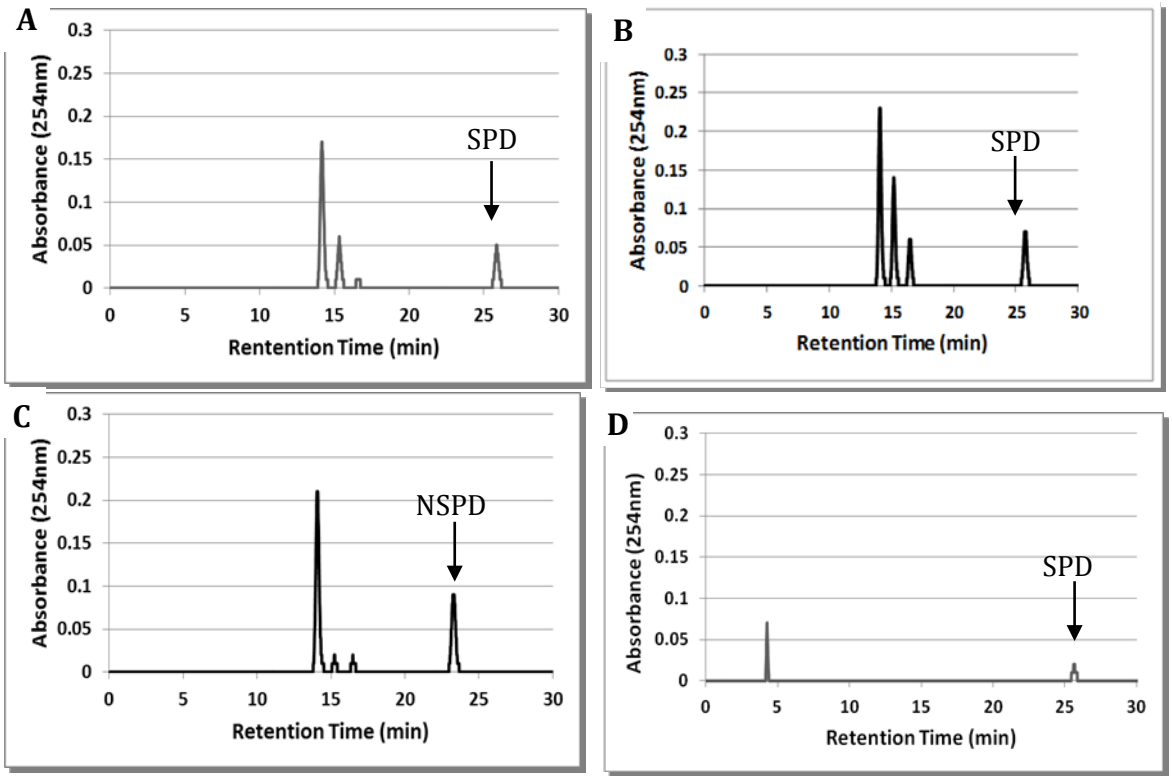


**Figure 16. HPLC of media conditions and *V. cholerae* Δ*nspC* mutant with added norspermidine. A)** HPLC chromatogram representative of the *V. cholerae* Δ*nspC* mutant with 1µM exogenous norspermidine. **B)** HPLC chromatogram of the *V. cholerae* Δ*nspC* mutant with 100 µM exogenous norspermidine. **C)** HPLC chromatogram the *V. cholerae* Δ*nspC* mutant with 1 mM exogenous norspermidine. The spermidine (SPD) peak is present at 1 µM and 100 µM norspermidine, but diminished and replaced with norspermidine (NSPD) at 1mM. **D)** HPLC chromatogram representing the polyamines present in the growth medium.

### *Identification of residues important for spermidine binding*

The PotD1 protein of *V. cholerae* shares a 62% identity with the PotD protein of *E. coli* as predicted by sequence alignment using ClustalW (Figure 17A). The PotD protein of *E. coli* has been extensively characterized both through the identification of amino acids involved in polyamine binding and the crystal structure of PotD complexed with spermidine (26, 38). The *V. cholerae* PotD1 protein was characterized by mutating amino acids which are conserved between the *E. coli* PotD and *V. cholerae* PotD1 and have been shown to be

strongly involved in the binding of spermidine to the *E. coli* PotD binding site (26). Sugiyama et *al.* classify this protein as having two dynamic domains with the binding cleft situated between these domains. The *E. coli* PotD cleft has four acidic residues (Glu 36, Asp 168, Glu 171, and Asp 257) that interact with protonated spermidine, and five aromatic side chains (Trp 34, Tyr 37, Trp 255, Tyr 293, and Trp 229) that anchor the carbon backbone through Van der Waals interactions (38), but the residues W34, E171, W255, and D257 were shown to have the most drastic effect on spermidine binding (26). The homology model of PotD1 suggests a similar topology and ligand interaction in *V. cholerae* (Figure 17 B and C). To determine where these amino acids might be located in the 3D structure of *V. cholerae* PotD1, I made use of a homology model. A 3D representation of the PotD1 protein in *V. cholerae* was modeled using the PotD protein of *E. coli* complexed with spermidine in the dimer form as a template (Figure 17B). A magnified view of the PotD1 binding cleft shows the amino acids that are conserved in PotD and have been shown to play an important role in interaction with spermidine at the binding cleft of PotD in *E. coli*. Therefore, I hypothesized that the following amino acid residues would contribute to the ability of PotD1 to bind spermidine and norspermidine: W32, E168, W252, and D254, which are identified with arrows in figures 17A and C (Figure 17 A and C). Kashiwagi et *al*. (26) reported that the tryptophan in *E. coli*, correlating to the W32 residue in *V. cholerae*, had decreased uptake activity of spermidine and putrescine binding. I hypothesized that this residue is stabilizing the polyamine binding due to the electrostatic interactions between the electron dense rings of tryptophan and the amine of the polyamine, and that altering the amino acid to a leucine would decrease polyamine binding but still confer some stability from the methyl groups of leucine. The E168 and D254 residues were changed to alanines to show that glutamic acid at

position 168 and aspartic acid at position 254 are directly involved in stabilization of the amine groups within the polyamine, and when there is only one methyl group from the alanine available for interaction with the ligand, binding should be reduced. The D254 residue was also altered to an asparagine to show that normal binding would be reduced due to the charge repulsion between the amine groups on asparagine and the polyamine. The W252 residue was altered to a leucine because it is thought that the tryptophan contributes to spermidine stability within the cleft due to the pi bonds interacting with the positively charged polyamine; and leucine, with two methyl groups, would be better tolerated in that position rather than alanine with one methyl group.

**A**

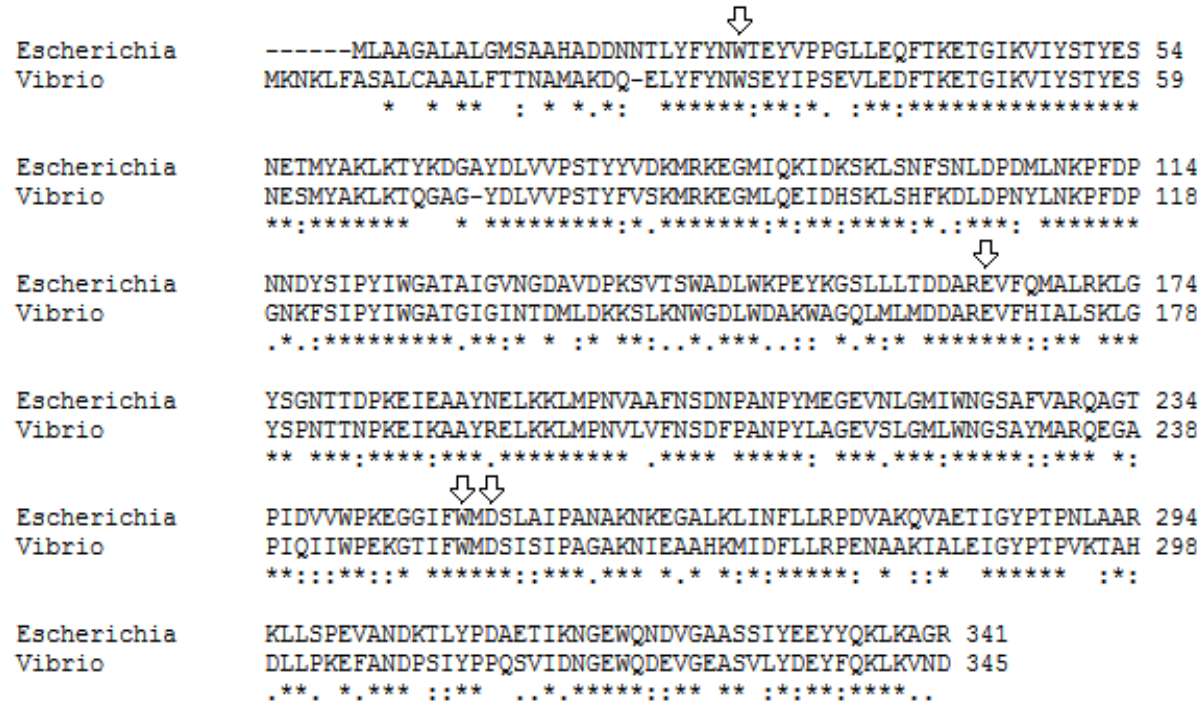

**B**

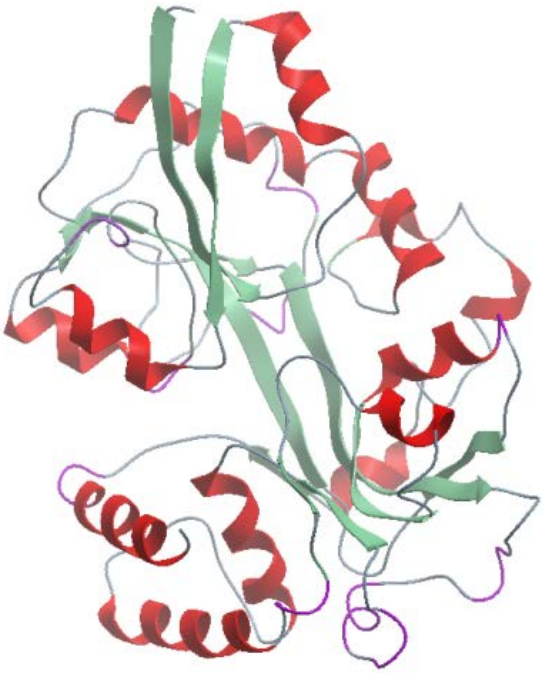

**C**

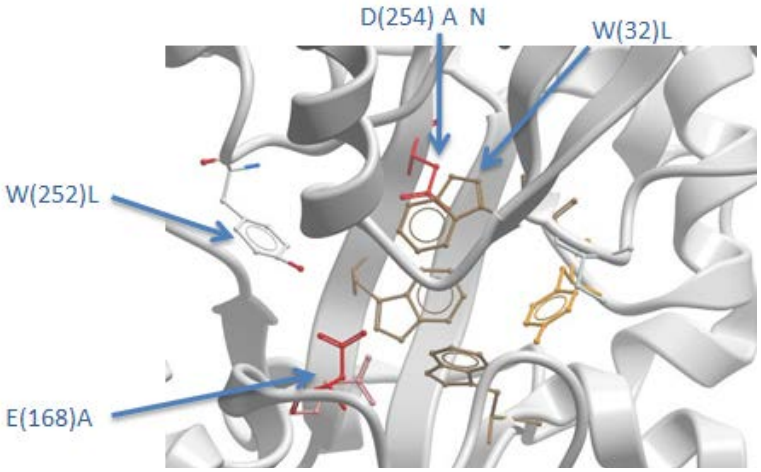


**Figure 17. PotD1 alignment and homology model. A)** The alignment of *V. cholerae* PotD1 and *E. coli* PotD proteins. The arrows indicate the homologous amino acid residues chosen for site-directed mutagenesis. **B)** The predicted PotD1 protein model. SWISS-MODEL was used for homology structure determination using 1POY as a template. MOLSOFT ICM Browser was used to depict structure. This image is colored by secondary structure, red = α-helices and green = β strands (38)**. C)** A magnified view of the PotD1 binding cleft modeling amino acid side chains that are predicted to have a direct impact on the ligand binding interaction of PotD1 as compared to the *E. coli* PotD (26). The amino acids chosen to have a direct impact in the *Vibrio* system are labeled.

***Construction of the potD1 mutants***

To further understand the role of certain amino acids within the PotD1 binding cleft, PCR mutagenesis was used to mutate specific residues within the *potD1* gene, corresponding to W32L, E168A, W252L, D254A, and D254N. Representative experimental data obtained during the construction of one of these mutants, W252L, is shown in figures 18-21. Mutagenic forward and reverse primers were designed to alter each amino acid residue (Table 3) and encoded complementary sequences that allowed the fusion of each amplified piece of the *potd1* gene (Figure 18). For example, each mutant was constructed by amplifying both upstream and downstream fragments using mutagenic and outside *potD1* primers, excised (Figure 19), and fused (Figure 20) using the outside *potD1* primers, PA 138 and PA144. The mutated genes were cloned into a pCR2.1 TOPO vector, transformed into *E. coli*, and the presence of *potD1* was confirmed using colony PCR (Figure 21); the presence of the mutation was confirmed by sequencing. The inserts were liberated from pCR2.1 and subcloned into pACYC184 as described in the Materials and Methods. Presence of the insert in pACYC184 was confirmed using colony PCR. A Western blot using the V5 epitope tag engineered to each mutant showed that the mutant genes expressed at the same level as the wild-type gene (Figure 22).

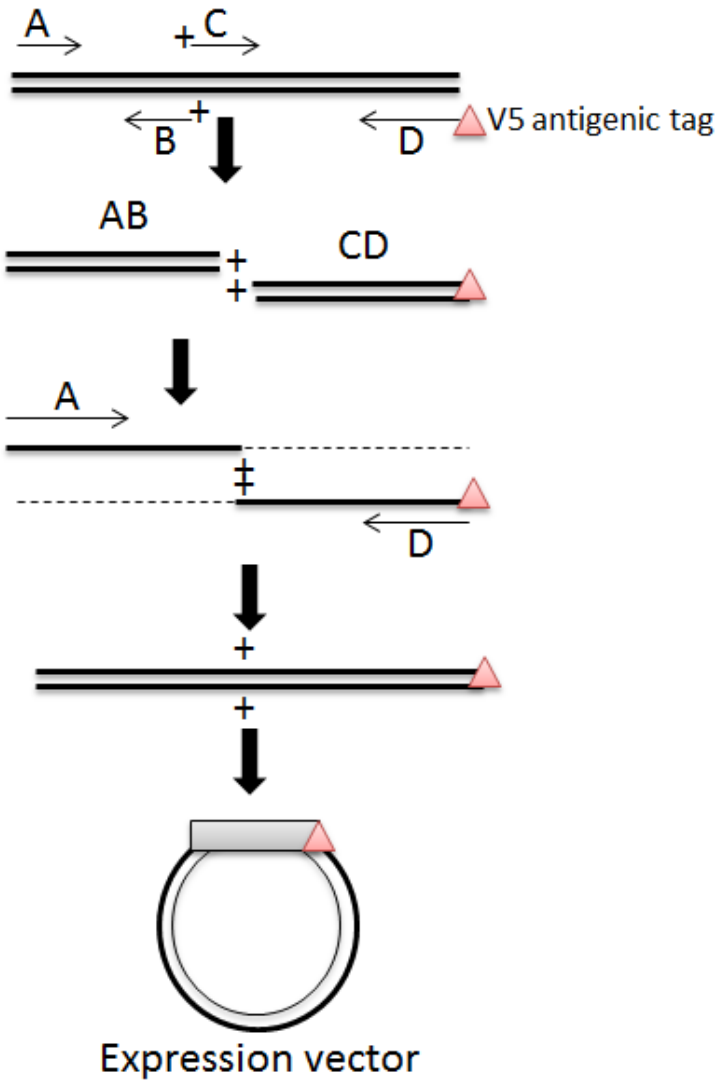


**Figure 18**. **Visual representation depicting PCR mutagenesis of each mutant.** The triangle on primer D represents an epitope tag engineered to the reverse primer for amplification of the *potD1* gene. The middle primers, B and C, represent the mutagenic primers encoding complementary regions for stitching together the PCR products. The mutants were first cloned into a pCR2.1 TOPO vector before being put into the pACYC184 vector.

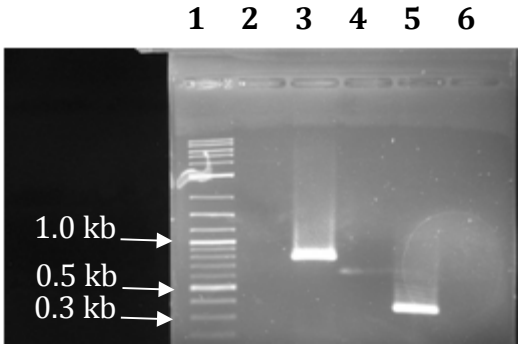


**Figure 19. Gel electrophoresis representing the W252L mutagenic fragments.** The first lane is the 2-log ladder. Lane 3 and 5 are representative of the upstream and downstream fragments. The rest of the lanes are empty.

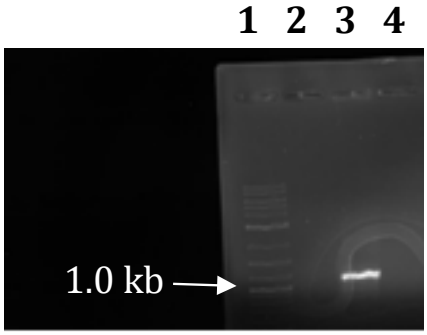


**Figure 20. Gel electrophoresis representing the W252L mutant *potD1* fused gene sequence**. Lane 1 is the 2-log ladder and lane 3 represents the 1100 bp fused mutant sequence.

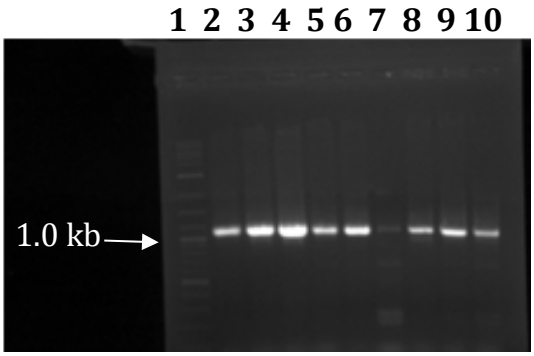


**Figure 21. Colony PCR of the W252L mutant in the pCR2.1 TOPO vector.** Colony PCR was performed using primers PA138 and PA144. The first lane is the 2-log ladder. The second lane is a positive control and the respective lanes are individual colonies.

***Mutations in the putative binding cleft residues do not alter expression***

Our results confirm that expression was uniform among all mutants. Comparison of wild-type PotD1 expression to mutant PotD1 expression showed that no difference in expression was noticed among the mutants (Figure 22).

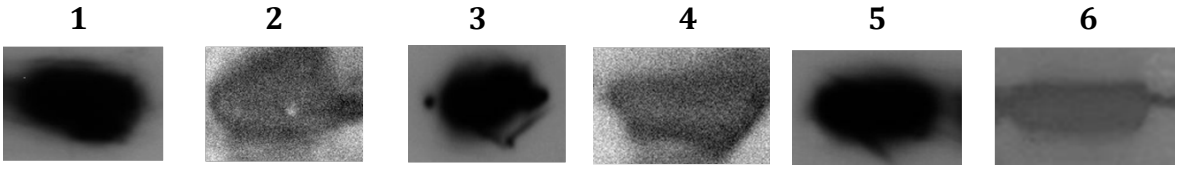


**Figure 22. Western Blot showing expression of PotD1 mutants.** Mutants were detected using the V5 epitope tag. The size of protein in each lane is 40 kDa. Lane 1 is the D254N mutant, Lane 2 is the D254A mutant, Lane 3 is the E168A mutant, Lane 4 is the W32L mutant, Lane 5 is the W252L mutant, and Lane 6 is the Δ*potD1* w/ PotD1.

***Mutations in the PotD1 binding cleft affect spermidine uptake***

To assess the effect of mutating the amino acid residues W32, E168, D254, and W252 on spermidine binding to PotD1, the intracellular spermidine levels were quantified in cells containing these protein variants (Figure 23). Spermidine levels in the Δ*potD1* strain, expressing the wild-type *potD1* gene from a medium copy plasmid (15-20 copies), were similar to those in the wild-type *V. cholerae* with a single chromosomal *potD1* gene. Because the pACYC184::*potD1* construct fully restored spermidine uptake, any reduction in the levels of spermidine containing the *potD1* mutants can be attributed to the mutations rather than other secondary factors (Figure 23). Therefore, the amount of spermidine in the mutants was compared to the complementation strain with wild-type PotD1 reintroduced into the Δ*potD1* strain (Table 4).

Mutations in the W252 amino acid residue were detrimental to the uptake of spermidine and the W252L mutant behaved similarly to the ΔPotD1 strain (Figure 23). The amount of intracellular spermidine was approximately 3% compared to the amount of

spermidine uptake supported by wild-type PotD1 (Table 4). The D254 amino acid residue was just as important in contributing to spermidine uptake (Figure 23). Spermidine import for D254N and D254A was 5% and 6% respectively, of the total intracellular spermidine uptake supported by the wild-type PotD1 (Table 4). In contrast, the W32 and E168 residues were not as important in spermidine binding, and these mutants were still able to support uptake of spermidine, although uptake was considerably decreased when compared to wild-type PotD1 (Figure 23); both W32L and E168A mutations allowed for only about 20% of spermidine uptake compared to wild-type PotD1 (Table 4). Thus, the W252L, D254A, and D254N mutations are detrimental to spermidine uptake and E168A and W32L mutations are more tolerated. These results suggest that W252 and D254 amino acids are the most important for spermidine binding to PotD1, and the E168 and W32 amino acids are of secondary importance.

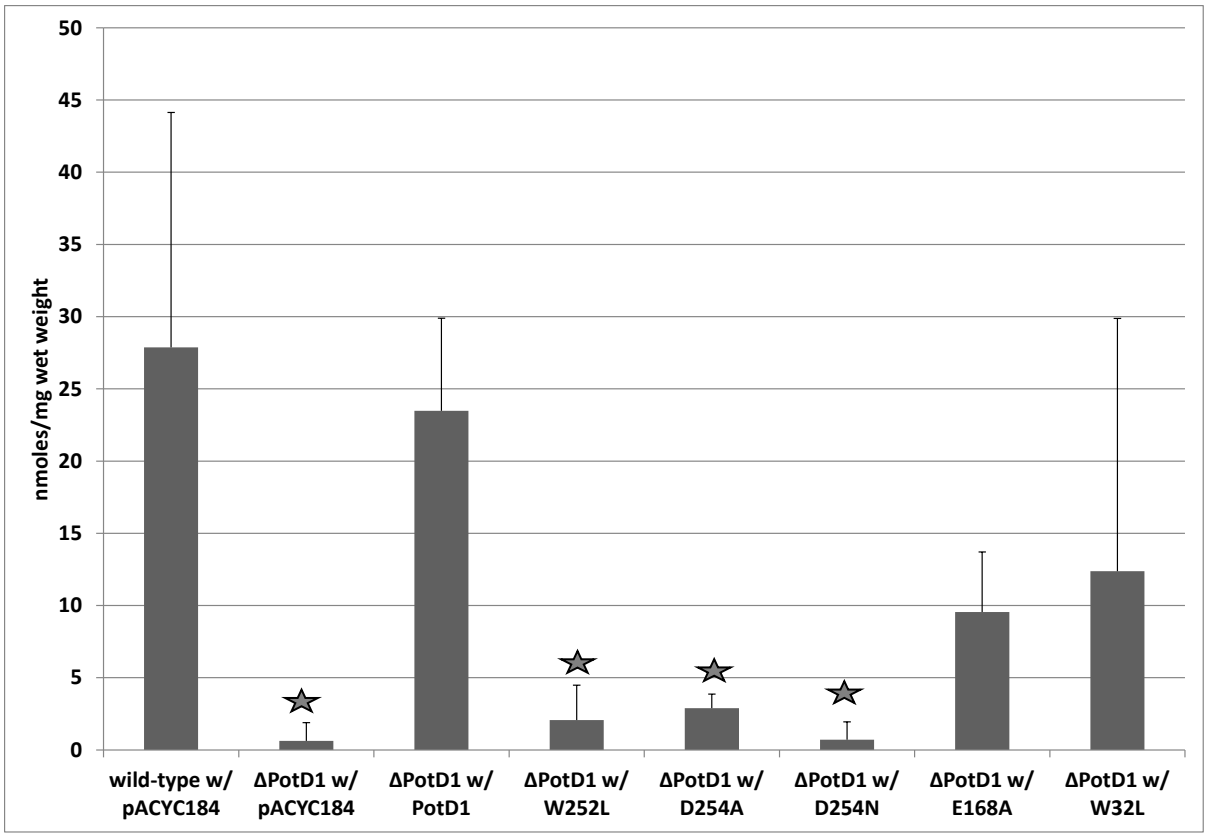


**Figure 23. Spermidine presence in wild-type and mutated PotD1 protein.** The average spermidine amounts present in cells containing wild-type or mutated PotD1 protein. Standard deviation is representative of multiple replicates (2-4 replicates). All strains contain either the empty pACYC184 vector or the same vector with the specified mutants cloned into it. A 2-tailed t-test was used to determine statistical significance of differences compared to Δ*potD1* w/ PotD1. Differences with p values less than 0.05 were deemed significant and are indicated with a star.

### *Mutations in potD1 alter the biofilm phenotype in V. cholerae*

Because PotD1 directly affects biofilm formation in *V. cholerae*, the biofilm phenotypes of the mutants were explored. If PotD1 is not present in *V. cholerae*, biofilm formation is drastically increased compared to wild-type *V. cholerae* (Figure 24). Because PotD1 is responsible for spermidine uptake, this result suggested intracellular spermidine presence was the key factor in biofilm formation. To determine if the ability of the mutants to uptake spermidine correlated with inhibition of biofilm formation, the effect of the mutations on biofilm formation was assessed. I hypothesized that the mutants that only allowed

minimal spermidine uptake, such as W252L, D254A, and D254N, would not complement the biofilm phenotype and would look similar to the Δ*potD1* strain. I also hypothesized that the mutations that allowed reduced uptake of spermidine, W32L and E168A, would lead to a partial complementation of biofilm phenotype. Biofilm formation among all of the mutants was increased, as compared to wild-type *V. cholerae* and also Δ*potD1* with PotD1. This increase is also seen in Δ*potD1,* albeit the increase is much higher compared to the mutants. Although the W252L, D254A, and D254N mutants are unable to uptake spermidine (Figure 23, Table 4), the biofilm formed does not increase to levels seen in the Δ*potD1* mutant, which would have been expected if spermidine was the only variable behind this biofilm phenotype. Overall, the biofilm phenotype of each mutant did not correlate to the expected biofilm phenotype based upon their ability to uptake spermidine, but the increase in biofilm formation compared to wild-type PotD1 does advocate that spermidine import plays a role in biofilm formation, considering all mutants are lacking in their ability to uptake spermidine (Figures 23 and 24). These results also suggest that spermidine, being bound by PotD1 and transported, may not be the only influence on biofilm formation in *V. cholerae* as previously seen. Instead the PotD1 protein may be playing a direct role in regulation of biofilm formation by a yet unidentified mechanism.

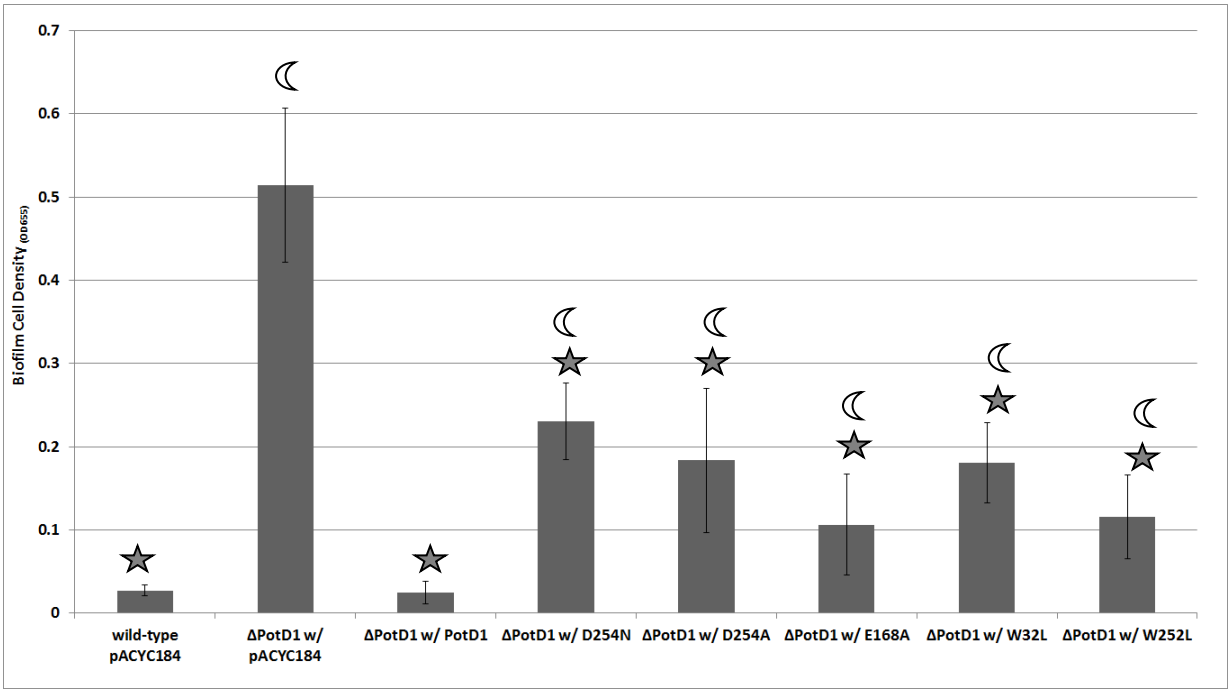


**Figure 24**. **Biofilm formation of PotD1 mutants, wild-type PotD1, and ΔPotD1.** Biofilm formation of PotD1 mutants is compared to wild-type PotD1 and a strain without PotD1. The biofilms were grown for 34 hours and this data is representative of four replicates. Error bars indicate standard deviation. A two-tailed t-test was used to determine if the differences seen are significant compared to Δ*potD1* w/ pACYC184, shown with gray stars, and to determine significance compared to Δ*potD1* w/ PotD1, shown with a crescent. Differences were deemed significant for p values less than 0.05.

Table 4. **Spermidine uptake and biofilm formation of each mutant and ΔPotD1 compared to wild-type PotD1. Numbers are given as averages with standard deviations.**

| | Spermidine uptake (% WT) | Biofilm (fold WT) |
|---|---|---|
| W32L | 20 +/- 17.5 | 7 +/- 0.05 |
| E168A | 20 +/- 4.2 | 4 +/- 0.06 |
| W252L | 3 +/- 2.42 | 4 +/- 0.05 |
| D254A | 6 +/- 1.0 | 7 +/- 0.09 |
| D254N | 5 +/- 4.8 | 5 +/- 0.05 |
| ΔPotD1 | 2 +/- 1.3 | 18 +/- 0.09 |

***Construction and purification of a periplasmic expression protein for potD1***

To determine the binding affinity of the PotD1 protein to its respective ligands, norspermidine and spermidine, a recombinant PotD1 expression protein was engineered using the pMAL Protein Fusion and Purification System (Figure 25). In this system the gene of interest is cloned into the above vector in frame with the maltose binding protein (MBP), enhancing the stability and solubility of foreign proteins expressed in *E. coli*.

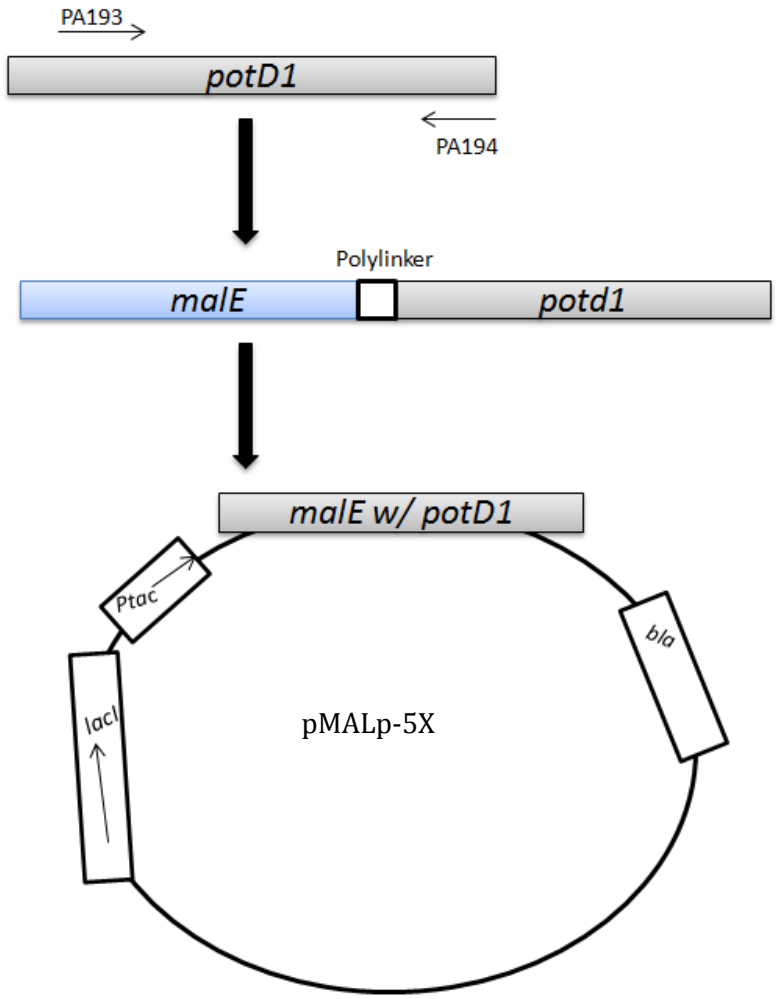


**Figure 25. Visual representation of the MBP-PotD1 fusion protein construction.** The *malE* sequence codes for the MBP protein. A polylinker joins the *malE* and *potd1* gene sequences. The *lacI* repressor and *Ptac* promoter sequences allow for induced transcription by the allolactose mimic, IPTG. The *bla* gene encodes ampicillin resistance.

The *potD1* gene was amplified using primers PA193 and PA194, and utilized the signal sequence of the pMAL-p5X vector for periplasmic localization (Figure 26). The *potD1* gene was restricted, purified, ligated into pMAL-p5X, and transformed into NEB *E. coli* (Figure 27). Presence of the insert was verified and a clone with the insert was sequenced to confirm correct construction. This plasmid was used for expression and purification of MBP-PotD1 fusion protein. A single band of ~ 80 kDa, corresponding to the expected molecular weight of the fusion protein, can be seen (Figure 28). Purification of the MBP-PotD1 fusion protein in polyamine deficient media was necessary and produced a purer periplasmic content (Figure 29). The mutant W252L PotD1 protein was also fused, in a similar manner, with the MBP protein as confirmed by the ~ 80 kDa band present in Figure 30; this mutant was chosen because of its diminished spermidine uptake and should not exhibit the same binding kinetics as wild-type PotD1. A Bradford assay and SDS page confirmed protein presence and these fractions were pooled and concentrated to 1 mg/mL (Figures 28-30).

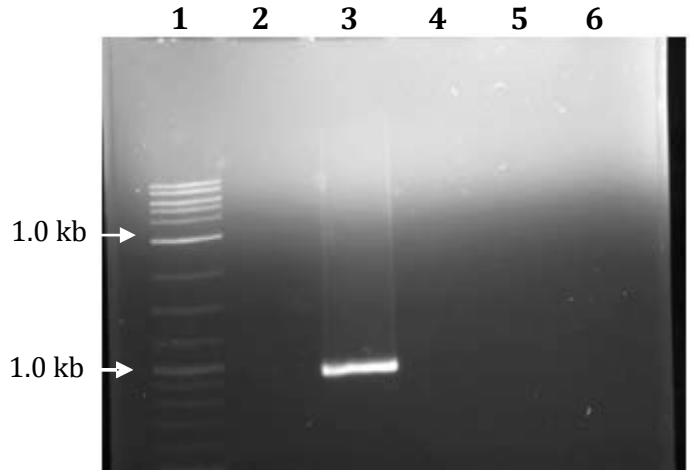


**Figure 26**. **Gel Electrophoresis of *potD1* without its signal sequence.** Lane 1 is the 2-log ladder and lane two represents the ~ 970 bp band.

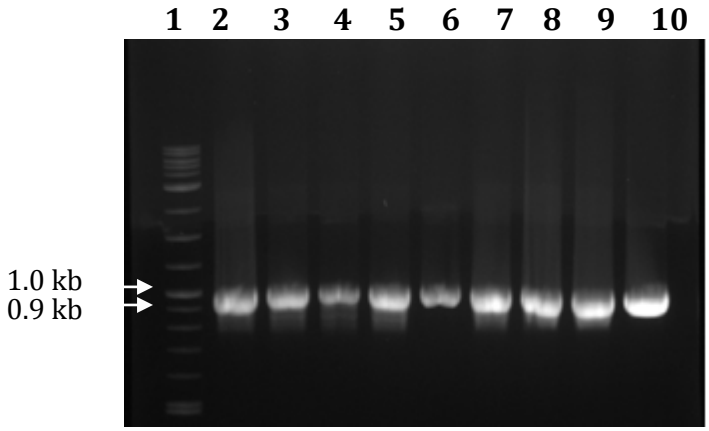


**Figure 27. Colony PCR confirming the *potD1* in the pMALp-5X vector.** Lane 1 is the 2-log ladder and lanes 3-10 represent individual colonies which are all positive for the insert.

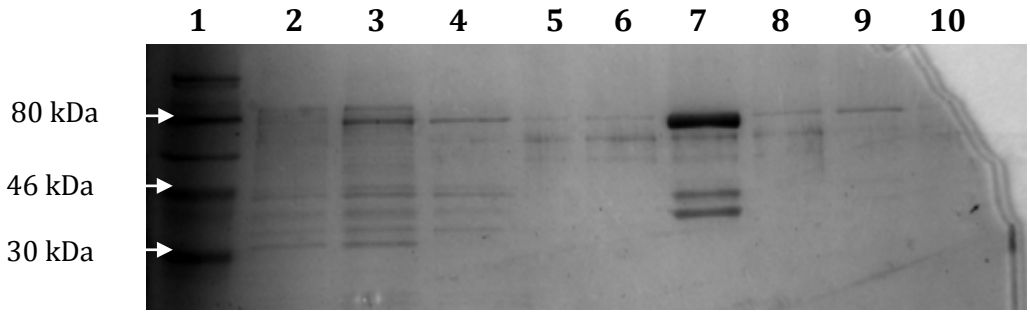


**Figure 28. Polyacrylamide denaturing gel of MBP-PotD1 expression and purification.** Lane 1 represents the ColorPlus Prestained Protein Marker (7-175 kDa), lane 2 is the uninduced cell extract, lane 3 is the induced cell extract, lane 4 is the column wash flow through, lanes 5-10 are fractions collected during purification.

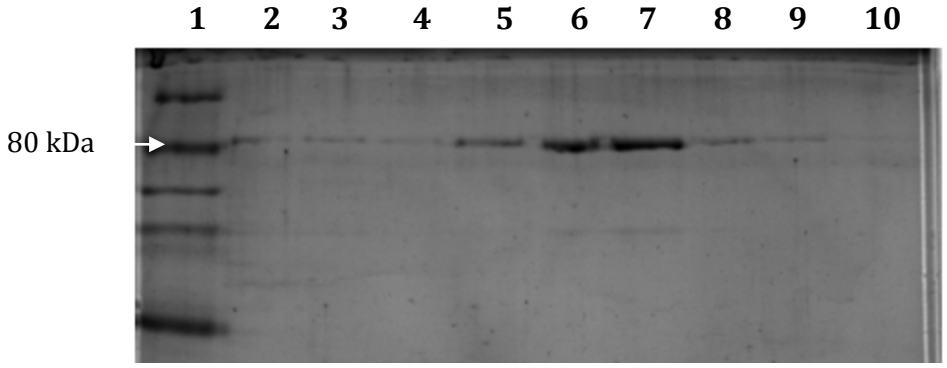


**Figure 29. Denaturing polyacrylamide gel of the MBP-PotD1 fusion protein in M9 minimal media.** Lane 1 represents the ladder and lanes 2-10 represent collected fractions containing the fusion protein. Fractions containing the fusion protein were pooled together and stored for further analysis.

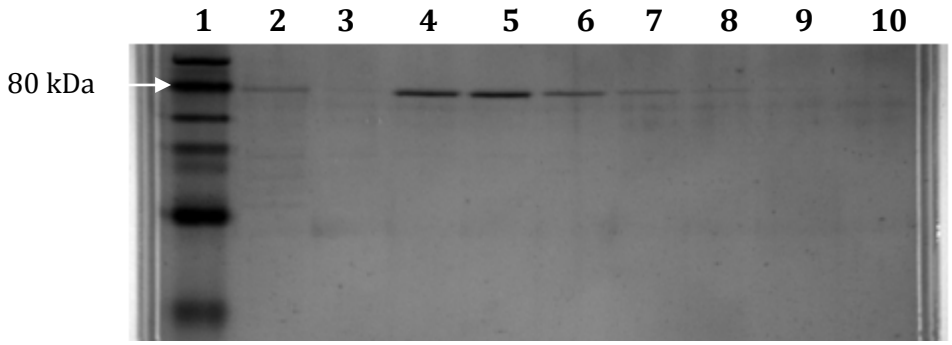


**Figure 30. Denaturing polyacrylamide gel of the MBP-W252L fusion protein in M9 minimal media.** Lane 1 represents the ladder and lanes 2-10 are the fractions containing the fusion protein. Fractions containing the fusion protein were pooled together and stored for further analysis.

***Determining the binding kinetics of PotD1***

Preliminary data with the PotD1 fusion protein, using Differential Scanning Flourimetry (DSF), shows stabilization with both norspermidine and spermidine (data not shown), suggesting PotD1 can bind both of these. However, Isothermal Titration Calorimetry (ITC) will be used to quantify the binding affinity of PotD1 to spermidine and norspermidine, if time permits. It is predicted that the PotD1 protein binding association will follow a 1:1 stoichiometric relationship with the ligand positioning itself in the predicted binding cleft of PotD1 (Figure 17). Determining the binding affinity of PotD1 to its ligands will allow for a more detailed characterization of the specificity that PotD1 possesses for both norspermidine and spermidine binding.

# DISCUSSION

The purpose of this study was to characterize the ability of the periplasmic PotD1 substrate binding protein to interact with spermidine and norspermidine, while exploring its influence on biofilm formation in the pathogen *V. cholerae.* This work establishes PotD1 as the first norspermidine transporter ever reported in any species. Previous results, in wild-type *V. cholerae,* demonstrated the potential competition of norspermidine to spermidine for binding to the PotD1 protein and presented the background for elucidating the role of PotD1 in *V. cholerae* (12). The importance of norspermidine to *V. cholerae* has been demonstrated and indicates the prominence of this molecule in varying aspects of *V. cholerae* physiology. The ability for PotD1 to uptake norspermidine indicates that this molecule is important enough to import from the extracellular environment, even when *V. cholerae* is able to synthesize norspermidine. Norspermidine can also act to upregulate biofilms (41), and growth and biofilm formation is impaired when *V. cholerae* is not able to synthesize norspermidine (24). The cellular need for norspermidine is also indicated by the ability of *V. cholerae* to utilize this molecule as the backbone in vibriobactin synthesis. The vibriobactin siderophore is used to scavenge and acquire ferric iron for various cellular processes and its performance is necessary to proper cell function (43, 44). Therefore, norspermidine is important for *V. cholerae* cell health. This research also demonstrates that PotD1 is the only norspermidine transporter as in the absence of PotD1 norspermidine transport is completely abolished.

Interestingly, while PotD1 is capable of transporting norspermidine, its preferred ligand is spermidine. *V. cholerae* does not synthesize much spermidine, although *nspC* can use putrescine under certain conditions instead of diaminopropane to synthesize spermidine instead of norspermidine. The lack of a robust spermidine synthesis pathway may lead to the hypothesis that *V. cholerae* does not utilize spermidine in cellular processes. However, the presence of a high affinity transport system that prefers spermidine over norspermidine argues against this hypothesis. It is likely that spermidine is an important molecule for *V. cholerae* and regulates aspects of its physiology that have not yet been determined. It is known that spermidine influences the cell in an opposite manner as norspermidine to regulate biofilms (11), but there may also be other intracellular effects that have yet to be elucidated.

This work also focused on understanding the PotD1 protein through a detailed biochemical characterization. A hypothesized model of the PotD1 protein predicts that the binding association will follow a 1:1 stoichiometric relationship with the ligand positioning itself in the predicted binding cleft of PotD1 between the N-terminus and C-terminus globular domains (35, 36, 37). Mutation of the W252 and D254 amino acid residues were detrimental to the binding of spermidine and the PotD1 proteins altered in these amino acids were still able to support uptake of spermidine, although uptake was considerably decreased (Figure 23). In contrast, the W32 and E168 residues were not as important in spermidine binding, and these mutants were still able to support uptake of spermidine, although uptake was considerably decreased when compared to wild-type PotD1 (Figure 23). Thus, the W252L, D254A, and D254N mutations are detrimental to spermidine uptake and E168A and W32L mutations are more tolerated. This suggests that the W252 and D254 amino acids are the most important for spermidine binding to PotD1 and the E168 and W32 amino acids are

of secondary importance. These results coincide with the biochemical characterization of the PotD protein in *E. coli*, with slight variations. The E171, W255, and D257 residues (analogous to E168, W252, and D254, of PotD1, respectively) were detrimental to spermidine binding in *E. coli* and W34 was used to a lesser extent (26). It is worth mentioning that the polyamine concentrations calculated in this mutant deviated drastically between the two trials performed and warrants another trial. Future experiments that are underway explore the effect of these mutations on norspermidine uptake and the relative affinities of PotD1 to spermidine and norspermidine using binding assays.

This work also attempted to investigate the link between spermidine uptake and biofilm formation using the various PotD1 mutants that were generated. Despite their inability to support spermidine uptake, the mutants were still able to suppress biofilm formation (Figure 24). This suggests that PotD1 may regulate biofilm formation through spermidine uptake, as well as a distinct yet unidentified mechanism. One possibility for the unidentified mechanism may involve interaction of PotD1 with other polyamines, such as norspermidine. ABC transporter function can vary greatly among different species and their architecture is reflective of the role they play within the cell with the substrate binding domain being essential to transporter function. The transport system has the capacity to regulate many physiological processes due to the cellular influence of transported substrate, but it cannot be ruled out that the protein itself is playing a direct regulatory role within the cell (45, 32, 46). An example of this includes the PotD1 protein. Interestingly, PotD of *E. coli* has been shown to regulate gene expression of the PotABCD operon (46). To further understand the unidentified mechanism that is influencing PotD1 to regulate biofilm formation, a future direction may include putting these mutants back onto the chromosome as

a single copy and then reanalyzing the biofilms. This would eliminate the interpretation that biofilm regulation of the mutants is affected due to the higher levels of mutant protein expression and perhaps secondary effects.

It is interesting to note that within the PotABCD2D1 system there are two hypothesized periplasmic binding proteins, PotD1 and PotD2. This is not an unusual characteristic considering multiple binding proteins with different binding specificities are able to utilize the same transporter system (47, 48). This work focused on understanding PotD1 function within the PotABCD2D1 system, but characterization of the whole system using bioinformatics allowed a more detailed understanding of PotD2 (Rutkovsky and Karatan, unpublished data), a very similar substrate binding protein as PotD1. This protein contains a sulphate/thiosulphate conserved binding site within the binding cleft, which may suggest sulfate transmembrane transporting activity. Interestingly, there are naturally occurring sulfonic acids within mammalian intestine such as taurine, and this molecule ($C_2H_7NO_3S$) could be a likely candidate for PotD2 binding considering the amine group situated at the end of the linear molecule. The effect of taurine on biofilm formation of prokaryotic species has not yet been explored but warrants further investigation.

Polyamines are essential molecules for most species, and this research also shows that PotD1 preferentially binds spermidine over norspermidine. Because norspermidine presence up-regulates biofilm formation (13) and spermidine presence decreases biofilm formation in *V. cholerae*, this suggests that PotD1 promotes polyamine uptake to regulate biofilm formation in environmental circumstances in which biofilm production is important: within the human host. The potential of this protein to alter binding function when norspermidine is present in high quantities illustrates the varying function this protein possesses to intake

molecules of necessity to the cell in certain circumstances. Although norspermidine concentration within the human intestine has not been characterized, dietary intake of polyamines to the gut lumen is on the order of about a millimolar per day (49), but polyamines such as spermidine are present in the micromolar range within the intestinal lumen (50, 51). This is especially interesting considering luminal polyamine content is being supplied at high concentrations yet present at low concentrations. This suggests that disappearance of polyamines from intestinal lumen may occur through rapid absorption, rapid degradation, or utilization *in situ* by both the human intestine and organisms that colonize this environment (52). It is thought that biofilm formation aids *V. cholerae* persistence in the stomach of the human host until the pathogen is able to reach the small intestine, which could suggest the role of PotD1 in recognition and uptake of polyamines in environments in which the polyamine content is considerably higher than the micromolar level, potentially the human stomach.

The overwhelming emphasis *V. cholerae* places on norspermidine use, through detection, uptake, and synthesis, illustrates the need for complex regulatory systems to maintain norspermidine balance. Recent work has demonstrated that elevated levels of *nspC* enhance *V. cholerae* biofilm formation without affecting intracellular norspermidine concentrations (13). This indicates the potential presence of a feedback mechanism maintaining norspermidine homeostasis in *V. cholerae*. Interestingly, NspS, the norspermidine sensor protein, also regulates biofilm formation similarly through interaction with norspermidine, yet this phenomenon is independent of *nspC* expression and offers an alternative input into the biofilm regulatory network (13).

It should be noted that recent work has demonstrated the use of norspermidine, but not closely related polyamines, to prevent biofilm formation in *B.subtilis*, *E. coli*, and *S. aureus* (53), but this does not seem to be the case regarding the ability of *V. cholerae* to utilize norspermidine in biofilm regulation. It has been known that polyamines are utilized by most species for regulation, but the role of norspermidine to enhance biofilm formation by *V. cholerae* and inhibit biofilm formation by others further demonstrates the diverse strategies that different species use to interact with their host environment.

The PotD protein is a known spermidine transporter in many species, including *E.coli*, *Y. pestis*, *S. pneumonia*, *Synechocystis sp*, *P. aeruginosa*, and *V. cholerae* (26, 16, 54, 55, 12), but PotD1 homology among a diverse range of prokaryotes from different environmental niches (Figure 4) suggests its importance in cellular feats as well as ancestral evolutionary presence. It was recently shown by Joshi et *al* that *S. aureus* USA300 and other bacterial species have lost their polyamine biosynthesis genes over the course of evolution (56), but interestingly this strain exhibits a homologous protein to *V. cholerae* PotD1 (Figure 4). This demonstrates that PotD in this species may be performing a similar role in binding multiple polyamines that are needed for proper cell function. The ancestral evolutionary presence of periplasmic binding proteins, like PotD1, demonstrates the potential of these proteins to perform specific yet varied cellular duties.

# REFERENCES


1. **Faruque SM, Biswas K, Udden SMN, Ahmad QS, Sack DA, Nair GB, Mekalanos JJ.** 2006. Transmissibility of cholera: in vivo-formed biofilms and their relationship to infectivity and persistence in the environment. Proc. Natl. Acad. Sci. U.S.A. **103**: 6350-5.

2. **Hung DT, Zhu J, Sturtevant D, Mekalanos JJ.** 2006. Bile acids stimulate biofilm formation in Vibrio cholerae. Mol. Microbiol. **59**: 193-201.

3. **Hoyle BD, Costerton JW.** 1991. Bacterial resistance to antibiotics: the role of biofilms. Prog. Drug Res. **37**: 91-105.

4. **Kierek-Pearson K, Karatan E.** 2005. Biofilm development in bacteria. Adv. Appl. Microbiol. **57**: 79-111.

5. **Seper A, et al.** 2011. Extracellular nucleases and extracellular DNA play important roles in *Vibrio cholerae* biofilm formation. Mol. Microbiol. **82**: 1015-37.

6. **Butler SM, Camilli A.** 2005. Going against the grain: chemotaxis and infection in *Vibrio cholerae*. Nat. Rev. Microbiol. **3**: 611-20.

7. **Zhu J, Mekalanos JJ.** 2003. Quorum sensing-dependent biofilms enhance colonization in *Vibrio cholerae*. Dev. Cell **5**: 647-56.

8. **Tamayo R, Patimalla B, Camilli A.** 2010. Growth in a biofilm induces a hyperinfectious phenotype in *Vibrio cholerae*. Infect. Immun. **78**: 3560-3569.

9. **Merrell DS, et al.** 2002. Host-induced epidemic spread of the cholera bacterium. Nature **417**: 642-5.

10. **Alam A, et al.** 2005. Hyperinfectivity of human-passaged *Vibrio cholerae* can be modeled by growth in the infant mouse. Infect. Immun. **73**: 6674-9.

11. **He H, Cooper JN, Mishra A, Raskin DM.** 2012. Stringent response regulation of biofilm formation in *Vibrio cholerae*. J. Bacteriol. **11**: 2962-72.

12. **McGinnis MW, Parker Z, Walter N, Rutkovsky A, Cartaya-Marin C, Karatan E.** 2009. Spermidine regulates *Vibrio cholerae* biofilm formation via transport and signaling pathways. FEMS Microbiol. Lett. **299**: 166-174.

13. **Parker ZM, Pendergraft SS, Sobieraj J, McGinnis MM, Karatan E.** 2012. Elevated levels of the norspermidine synthesis enzyme NspC enhance *Vibrio cholerae* biofilm formation without affecting intracellular norspermidine concentrations. FEMS Microbiol. Lett. **329**: 18-27.

14. **Merrell DS, Camilli A.** 1999. The cadA gene of *Vibrio cholerae* is induced during infection and plays a role in acid tolerance. Mol. Microbiol. **34**: 836-49.

15. **Yoshida M, et al.** 2004. A unifying model for the role of polyamines in bacterial cell growth, the polyamine modulon. J. Biol. Chem. **279**: 46008-13.

16. **Ware D, Jiang Y, Lin W, Swiatlo E.** 2006. Involvement of potD in *Streptococcus pneumoniae* polyamine transport and pathogenesis. Infect. Immun. **74**: 352-61.

17. **Eraso JM, Kaplan S.** 2009. Regulation of gene expression by PrrA in *Rhodobacter sphaeroides* 2.4.1: role of polyamines and DNA topology. J. Bacteriol. **191**: 4341-52.

18. **Wortham BW, Oliveira MA, Fetherston JD, Perry RD.** 2010. Polyamines are required for the expression of key Hms proteins important for *Yersinia pestis* biofilm formation. Environ. Microbiol. **12**: 2034-47.

19. **Terui Y, et al.** 2010. Ribosome modulation factor, an important protein for cell viability encoded by the polyamine modulon. J. Biol. Chem. **285**: 28698-28707.

20. **Higashi K, et al.** 2008. Selective structural change by spermidine in the bulged-out region of double-stranded RNA and its effect on RNA function. J. Biol. Chem. **283**: 32989-32994.

21. **Yoshida M, Meksuriyen D, Kashiwagi K, Kawai G, Igarashi K.** 1999. Polyamine stimulation of the synthesis of oligopeptide-binding protein (OppA). Involvement of a structural change of the Shine-Dalgarno sequence and the initiation codon aug in oppa mRNA. J. Biol. Chem. **274**: 22723-8.

22. **Kusama-Eguchi K, Irisawa M, Watanabe S, Watanabe K, Igarashi K.** 1991. Increase in fidelity of rat liver Ile-tRNA formation by both spermine and the aminoacyl-tRNA synthetase complex. Arch. Biochem. Biophys. **288**, 495-9.

23. **Hetrick B, et al.** 2010. Polyamines accelerate codon recognition by transfer RNAs on the ribosome. Biochemistry **49**: 7179-7189.

24. **Lee J, et al.** 2009. An alternative polyamine biosynthetic pathway is widespread in bacteria and essential for biofilm formation in *Vibrio cholerae*. J. Biol. Chem. **284**: 9899-9907.

25. **Ames GF.** 1986. Bacterial periplasmic transport systems: structure, mechanism, and evolution. Annu. Rev. Biochem. **55**: 397-425.

26. **Kashiwagi K, et al.** 1996. Spermidine-preferential uptake system in *Escherichia coli*. J. Biol. Chem. **271**: 12205-12208.

27. **Igarashi K, Kashiwagi K.** 2010. Modulation of cellular function by polyamines. Int. J. Biochem. Cell Biol. **42**: 39-51.

28. **Higashi K, et al.** 2010. Identification and functions of amino acid residues in PotB and PotC involved in spermidine uptake activity. J. Biol. Chem. **285**: 39061-39069.

29. **Furuchi T, Kashiwagi K, Kobayashi H, Igarashi K.** 1991. Characteristics of the gene for a spermidine and putrescine transport system that maps at 15 min on the *Escherichia coli* chromosome. J. Biol. Chem. **266**: 20928-33.

30. **Russell RR, Aduse-Opoku J, Sutcliffe IC, Tao L, Ferretti JJ.** 1992. A binding protein-dependent transport system in *Streptococcus* mutans responsible for multiple sugar metabolism. J. Biol. Chem. **267**: 4631-7.

31. **Kashiwagi K, Miyamoto S, Nukui E, Kobayashi H, Igarashi K.** 1993. Functions of potA and potD proteins in spermidine-preferential uptake system in *Escherichia coli*. J. Biol. Chem. **268**: 19358-63.

32. **Shah P, Romero DG, Swiatlo E.** 2008. Role of polyamine transport in *Streptococcus pneumoniae* response to physiological stress and murine septicemia. Micro. Path. **45**: 167-172.

33. **Shah P, Nanduri B, Swiatlo E, Ma Y, Pendarvis, K.** 2011. Polyamine biosynthesis and transport mechanisms are crucial for fitness and pathogenesis of *Streptococcus pneumoniae*. Microbiology **157**: 504-15.

34. **Cui J, Davidson AL.** 2011. *Essays in Biochemistry ABC Transporters*. **F.J. Sharom.** (Portland Press Limited: London U.K).

35. **Quiocho FA.** 1990. Atomic structures of periplasmic binding proteins and the high-affinity active transport systems in bacteria. Philos. Trans. R. Soc. Lond., B, Biol. Sci. **326**: 341-52.

36. **Holland I.** 2003. *ABC proteins: from bacteria to man*. (Elsevier Science: Hong Kong).

37. **Davidson AL, Dassa E, Orelle C, Chen J.** 2008. Structure, function, and evolution of bacterial ATP-binding cassette systems. Microbiol. Mol. Biol. Rev. **72**: 317-64.

38. **Sugiyama S, et al.** 1996. The 1.8-A X-ray structure of the *Escherichia coli* PotD protein complexed with spermidine and the mechanism of polyamine binding. Prot. Sci. **5**: 1984-1990.

39. **Metcalf WW, et al.** 1996. Conditionally replicative and conjugative plasmids carrying l*acZ* for cloning, mutagenesis, and allele replacement in bacteria. Plasmid **35:** 1-13.

40. **Morgan DM**. 1998. *Polyamine Protocols. (*Humana Press: Totowa).

41. **Karatan E, Duncan TR, Watnick PI.** 2005. NspS, a predicted polyamine sensor, mediates activation of *Vibrio cholerae* biofilm formation by norspermidine. J. Bacteriol. **187:** 7434-7443.

42. **McGinnis M.** 2009.V*ibrio cholerae biofilm formation is regulated by polyamine biosythesis and transport.* (Appalachian State University: Boone, NC).

43. **Griffiths GL, Sigel SP, Payne SM, Neilands JB.** 1984. Vibriobactin, a siderophore from *Vibrio cholerae*. J. Biol. Chem. **259:** 383-5.

44. **Henderson DP, Payne SM.** 1994. *Vibrio cholerae* iron transport systems: roles of heme and siderophore iron transport in virulence and identification of a gene associated with multiple iron transport systems. Infect. Immun. **62:** 5120-5.

45. **Shah P, Swiatlo E**. 2008. A multifaceted role for polyamines in bacterial pathogens. Mol. Microbiol. **68:** 4-16.

46. **Antognoni F, et al.** 1999. Transcriptional inhibition of the operon for the spermidine uptake system by the substrate-binding protein PotD. J. Biol. Chem. **274:** 1942-8.

47. **Higgins CF, Ames GF.** 1981. Two periplasmic transport proteins which interact with a common membrane receptor show extensive homology: complete nucleotide sequences. Proc. Natl. Acad. Sci. U.S.A. **78:** 6038-42.

48. **Park JT, Raychaudhuri D, Li H, Normark S, Mengin-Lecreulx D.** 1998. MppA, a periplasmic binding protein essential for import of the bacterial cell wall peptide L-alanyl-gamma-D-glutamyl-meso-diaminopimelate. J. Bacteriol. **180:** 1215-23.

49. **Bardocz S, Grant G, Brown S, Ralph A, Pusztai A**. 1992. Polyamines in food - implications for growth and health. J. Nut. Biochem. **4:** 66-71.

50. **Bartos D, Campbell RA, Bartos F, Grettie DP.** 1975. Direct determination of polyamines in human serum by radioimmunoassay. Cancer Res. **35:** 2056-60.

51. **Bartos F, Bartos D, Grettie DP, Campbell RA.** 1977. Polyamine levels in normal human serum. Comparison of analytical methods. Biochem. Biophys. Res. Commun. **75:** 915-9.

52. **Milovic V.** 2001. Polyamines in the gut lumen: bioavailability and biodistribution. Eur J Gastroenterol. Hepatol. **13:** 1021-5.

53. **Kolodkin-Gal I, et al.** 2012. A self-produced trigger for biofilm disassembly that targets exopolysaccharide. Cell **149:** 684-92.

54. **Brandt AM, et al**. 2010. Characterization of the substrate-binding PotD subunit in Synechocystis sp. strain PCC 6803. Arch. Microbiol. **192:** 791-801.

55. **Wu D, et al.** 2012. Structural basis of substrate binding specificity revealed by the crystal structures of polyamine receptors SpuD and SpuE from *Pseudomonas aeruginosa.* J. Mol. Biol. **416:** 697-712

56. **Joshi GS, Spontak JS, Klapper DG, Richardson AR**. 2011. Arginine catabolic mobile element encoded speG abrogates the unique hypersensitivity of *Staphylococcus aureus* to exogenous polyamines. Mol. Microbiol. **82:** 9-20.

57. **Miller V, et al.** 1988. A novel suicide vector and its use in construction of insertion mutations: osmoregulation of outer membrane proteins and virulence determinants in *Vibrio cholerae* requires toxR. J. Bacteriol. **170:** 2575-83.

58. **Waldor MK, et al.** 1994. *Vibrio cholerae* O139 specific gene sequences. Lancet **343**.

59. **Haugo AJ, et al.** 2002. *Vibrio cholerae* CytR is a repressor of biofilm development. Mol. Microbiol. **45:** 471-83.

60. **Datsenko KA, et al.** 2000. One-step inactivation of chromosomal genes in *Escherichia coli* K-12 using PCR products. Proc. Natl. Acad. Sci. U.S.A. **97:** 6640-5.

# BIOGRAPHICAL SKETCH

Alexandria Colett Rutkovsky was born in Des Plaines, IL on September 21, 1988. After attending high school at Mooresville Senior High School in Mooresville, NC, she obtained a Bachelor of Science in Chemistry from Appalachian State University with a minor in biology. She began working in Dr. Ece Karatan's laboratory in 2008, where she realized her passion for research. Upon completion of her Master of Science in Biology at Appalachian State University in 2012, she will pursue her doctoral degree at the Medical University of South Carolina.